This manuscript is a pre-print and has not yet undergone peer review. It will be submitted to the conference proceedings of the EGC1 conference in Aberdeen, May 2023. The authors appreciate any thoughts and feedback, and can be contacted at conor.osullivan1@ucdconnect.ie or conor.osullivan@jacobs.com.

Subsurface storage capacity in underexplored sedimentary basins: Hydrogen and carbon dioxide storage on the Irish Atlantic margin

Conor M. O'Sullivan[1,2,3]; Pablo Rodriguez-Salgado[2,3]; Conrad Childs[2,3]; Patrick M. Shannon[2,4]

1 Jacobs, 160 Dundee Street, Edinburgh, EH11 1DQ, United Kingdom
2 Irish Centre for Research in Applied Geoscience (ICRAG), University College Dublin, Belfield, Dublin 4, Ireland
3 Fault Analysis Group, School of Earth Sciences, University College Dublin, Belfield, Dublin 4, Ireland
4 School of Earth Sciences, University College Dublin, Belfield, Dublin 4, Ireland

Abstract

As Ireland looks westwards to its Atlantic coastline to develop its renewable energy ambitions, offshore sedimentary basins on the Irish Atlantic margin offer significant potential for either collaborative energy (*e.g.* hydrogen, H_2) or carbon dioxide (CO_2) storage. Methodologies for subsurface storage assessment developed for basins with dense data coverage are typically less applicable to underexplored sedimentary basins. Therefore, a workflow is presented for subsurface storage assessment in underexplored basins which uses existing datasets to identify structural traps and populate a gas-in-place equation. This workflow is then applied to the Irish Atlantic margin; The geology of the Slyne, Erris, and Donegal basins is reviewed to understand their potential for subsurface storage. Jurassic, Triassic and Carboniferous reservoirs are investigated to understand their reservoir quality, extent, and the integrity of related seals. Structural trap types within the study area are then described and the storage assessment workflow is applied to three candidate sites with varying levels of data coverage. Across these three sites, P50 storage volumes equivalent to 720 million tonnes of CO_2 or 318 terawatt hours of H_2 are estimated. The results highlight the potential for underexplored sedimentary basins on the Irish Atlantic margin to support the deployment of offshore renewable energy projects and reduce Ireland's CO_2 emissions. This workflow is applicable to a variety underexplored sedimentary basins with limited data coverage and emphasises the utility of legacy hydrocarbon datasets for early-stage subsurface storage assessment.

1. Introduction

There is a growing recognition for the need to reduce the atmospheric concentration of carbon dioxide (CO_2) to slow the effects of climate change and to support the development of renewable energy sources by storing excess power. Many sedimentary basins which host prolific hydrocarbon resources are now being reassessed for their potential role as subsurface storage sites, including the North Sea and the Gulf of Mexico (Holloway *et al.*, 2006; Godec *et al.*, 2011; Agartan *et al.*, 2018). This is being done using data originally collected for the exploration and development of hydrocarbon resources, now repurposed to characterise subsurface storage sites. Subsurface storage is a key component in the reduction of atmospheric concentrations of CO_2 (Metz *et al.*, 2005; IPCC 2022) and also represents a technologically proven method to capture excess energy generated by renewable sources as rapidly deployable kinetic energy using compressed air energy storage (CAES) or as gaseous fuels such as hydrogen (H_2) (*e.g.* Takahashi *et al.*, 2009; Lech *et al.*, 2016; Ramos *et al.*, 2021).

The two basins mentioned above are host to prolific petroleum systems and have been the focus of intense hydrocarbon exploration and extraction activities for several decades. Methodologies for subsurface storage assessment have been developed for these basins which typically rely on dense grids of wells and 3D seismic reflection data (*e.g.* Lloyd *et al.* 2021). These workflows are not optimally applicable to the greater number of underexplored sedimentary basins which typically have far less well data and limited 3D seismic reflection data coverage. To remedy this, a workflow is presented in this study suitable for subsurface storage assessment in basins with more limited data coverage, which uses existing subsurface datasets in the form of well and seismic reflection data to populate an industry-standard Gas-in-Place equation.

This study outlines a methodology for estimating subsurface storage volumes in structural traps which can be applied to sedimentary basins with a variety of data coverage, from high-density 3D surveys to low density 2D grids of seismic reflection data and accompanying borehole data. This workflow is applied to three underexplored sedimentary basins offshore north-western Ireland. The lithological units which make up the most promising storage candidates within these basins are characterised and assessed for their potential as energy or CO_2 storage reservoirs. Storage structure types observed within the study area are then described, and the volumetric assessment workflow is then applied to three candidate storage sites with varying levels of data coverage, from 3D seismic reflection and well data coverage to low density 2D seismic lines and sparse well data. Finally, we discuss additional reservoirs on the Irish Atlantic margin which may warrant further study, briefly compare the geology of the Irish Atlantic margin to the basins offshore southern and eastern Ireland and discuss possible synergies with offshore renewable infrastructure development.

The results build upon previous assessments of hydrocarbon prospectivity (*e.g.* Trueblood, 1992; Spencer & MacTiernan, 2001; Scotchman *et al.*, 2018) and carbon dioxide storage potential (*e.g.* Lewis *et al.*, 2009) of the basins on the Irish Atlantic margin with a thorough analysis of the different reservoir formations and the identification of multiple potential structural storage sites worthy of further investigation. The workflow can also be applied to other basins offshore Ireland and further afield, particularly in locations with more limited subsurface data coverage. Renewable energy planning and development is at a nascent stage

offshore Ireland (Lange *et al.*, 2018; Roux *et al.*, 2022); the results of this study will ensure policy makers, renewable energy developers and power providers have a firm grasp of the opportunities that lie beneath the seabed.

2. Subsurface Gas Storage

There are many economic and societal reasons for storing gases in the subsurface. This study focuses on two uses:

- Reduction of atmospheric concentrations of CO_2 through capturing the greenhouse gas and storing it in subsurface reservoirs over geological timescales.
- Storage of energy, typically during periods when generation exceeds demand, which can be readily accessed as demand increases.

These are explored in more detail below.

2.1. CO_2 Storage

CO_2 can be captured using a variety of techniques, including directly at high-intensity sources like thermal power stations and cement plants, or from the atmosphere in lower concentrations using Direct Air Capture (DAC) methods (Bui *et al.*, 2018; Ringrose, 2020). There are several ways to store CO_2 underground, including precipitating it in a solid carbonate mineral such as calcium carbonate ($CaCO_3$) in basaltic rocks (*e.g.* Pogge von Strandmann *et al.*, 2019) or storing it as a fluid in either saline aquifers, depleted oil and gas fields and other structural traps (*e.g.* Bickle, 2009; Eiken *et al.*, 2011; Ringrose, 2020; Osmond *et al.*, 2022). This study will focus on the storage of CO_2 as a fluid in structural traps (Fig. 1A).

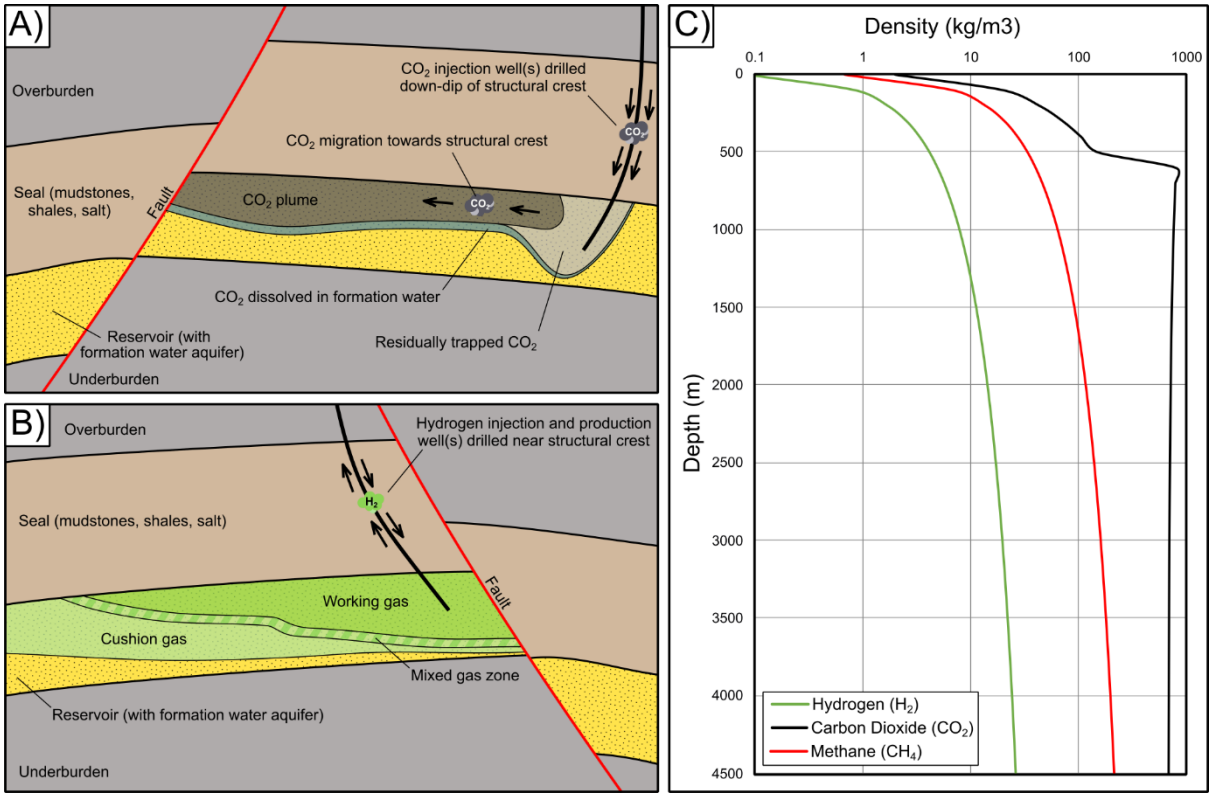

Figure 1: A) Schematic overview of CO_2 storage in structural traps. B) Schematic overview of H_2 storage in structural traps. C) Density changes of H_2, CO_2 and CH_4 (natural gas) with increasing depth. Calculated

using correlations from Lindstrom & Mallard (2022), the geothermal gradient of the Slyne Basin (31°C/km), and a hydrostatic pressure gradient (100 Bar/km).

CO_2 is typically stored at depths greater than 800-1000m underground. At these depths the ambient temperature and pressure is above the critical point of CO_2 (31 °C and 73-74 bar) which makes CO_2 a supercritical fluid (Ringrose, 2020). In this supercritical state CO_2 behaves in a unique way, with properties of both a liquid and a gas. Crucially, it has a much higher density than at atmospheric conditions (Fig. 1C), meaning a greater amount of CO_2 can be stored in the same volume at depth than on the surface. Supercritical CO_2 also has the viscosity of a gas, meaning it can flow into and through a porous storage medium more easily (Bui *et al.*, 2018; Ringrose, 2020). To have a meaningful impact on the effects of climate change, CO_2 must be stored in this manner for long periods of time (10,000+ years) with reasonable guarantees of storage integrity (Metz *et al.*, 2005; Bui *et al.*, 2018; IPCC 2022).

2.2. Energy Storage

Energy storage involves capturing and storing energy so that it can be used at a later time. Capturing energy generated during periods of low demand to be used later during periods of higher demand is an effective way to meet energy demand, balance input to national grids and ensure security of supply. With the increasing adoption of cleaner renewable energy, such as wind and solar which are inherently variable in nature, comes a requirement for a reliable and rapidly deployable back-up sources of energy. At present this is met primarily by natural gas supplies. However, the excess energy generated by renewable sources at times when demand is lower typically currently goes unused. With appropriate energy storage technologies and reservoirs, this excess energy could be stored for later use when demand exceeds wind, wave, or solar energy production.

The grid-scale energy storage technologies with the greatest capacity currently in operation are pumped-storage hydroelectric dams. Hydroelectric energy storage requires suitable topography and a source of water (Edwards, 2003). Other grid-scale storage solutions include large chemical batteries, but these require a significant supply of raw-materials, often sourced through environmentally damaging and exploitative processes (Wall *et al.*, 2017), and are currently typically capable of providing power for only a few hours at most. Alternatively, energy can be stored in the form of fluids in subsurface reservoirs. Currently, methane (*i.e.* natural gas) is the most commonly stored gas in subsurface reservoirs. In Ireland, the Southwest Kinsale gas field in the North Celtic Sea Basin was used as a storage facility for natural gas between 2001 and 2017 but has since been decommissioned (PSE Kinsale Energy, 2022).

In a similar manner to natural gas storage, other gaseous fuels can be generated using excess renewable energy and stored underground for later combustion, in a method known as Power-to-Gas (P2G). The several gases have been proposed for this purpose, including hydrogen (H_2) and ammonia (NH_3). This study will focus on hydrogen. Hydrogen is commonly categorised into a series of colours based on how it is produced (Dincer, 2012; Dawood *et al.*, 2020; Newborough and Cooley, 2020). The most common colours are listed below:

- Grey hydrogen: produced using steam methane reforming where water vapour (H_2O) is combined with natural gas (CH_4) at high pressures in the presence of a catalyst to produce hydrogen and carbon monoxide (CO). Further reaction occurs between the

carbon monoxide and water vapour in a water-gas shift reaction to produce additional hydrogen and carbon dioxide (CO_2). This is currently the most common production method.

- Blue hydrogen: produced using the same methods as grey hydrogen but the CO_2 is captured and stored rather than being emitted.
- Green hydrogen: produced using renewable energy to power the electrolysis of water (H_2O) to produce hydrogen and oxygen (O_2).

In the case of green hydrogen both the production and combustion of this gas produces no CO_2, highlighting its potential to decarbonise power generation (Dincer, 2012). However, while hydrogen has a higher energy content than natural gas, it is significantly less dense that natural gas (Heinemann *et al.*, 2018). Therefore, significant subsurface storage volume will be required to meet grid-scale energy demand currently provided by fuels like natural gas (Heinemann *et al.*, 2018; Crotogino, 2022; Duffy *et al.*, 2023). This lower density also makes hydrogen more buoyant that the formation water in subsurface sandstone reservoirs, leading to it migrating to the surface unless stored in a structural trap (Fig. 1B). Other properties of hydrogen, including its diffusivity, smaller molecular size and wettability properties indicate the importance of detailed seal characterisation when planning to store this gas in structural traps (Iglauer, 2022; Miocic *et al.*, 2023).

3. Dataset and Methodology

3.1 Dataset

A significant amount of subsurface data was collected by a variety of companies in the search for hydrocarbon accumulations (Naylor, 1983; Shannon, 2018) which can be used to understand the storage potential of different reservoir formations in the Slyne, Erris and Donegal basins. These basins are chosen as the focus for the present study as they lie relatively close to the Irish mainland and are in somewhat shallower water by comparison to the larger, deeper water and more oceanward Porcupine and Rockall basins. The database comprises seismic reflection data, tied to several exploration, appraisal and development wells and shallow boreholes. The 2D seismic database consists of 25 surveys acquired between 1975 and 2014 which totalled over 49,000 km in line-length (Fig. 2). The 3D seismic database consists of 12 surveys, acquired between 1997 and 2013, covering a total area in excess of 6000 km^2, although there is some survey overlap in the Northern Slyne Sub-basin (Fig. 2). Some of these surveys were reprocessed in 2006, 2012 and 2018. Seismic data is presented in European polarity, where a downward decrease in acoustic impedance corresponds to a negative (blue) reflection event and an increase in corresponds to a positive (red) reflection event. Seismic and geoseismic sections are vertically exaggerated by a factor of three. In the geoseismic sections, ball-ends are used to highlight where a fault terminates within a certain stratigraphic package, while faults without ball-ends are truncated by a younger surface.

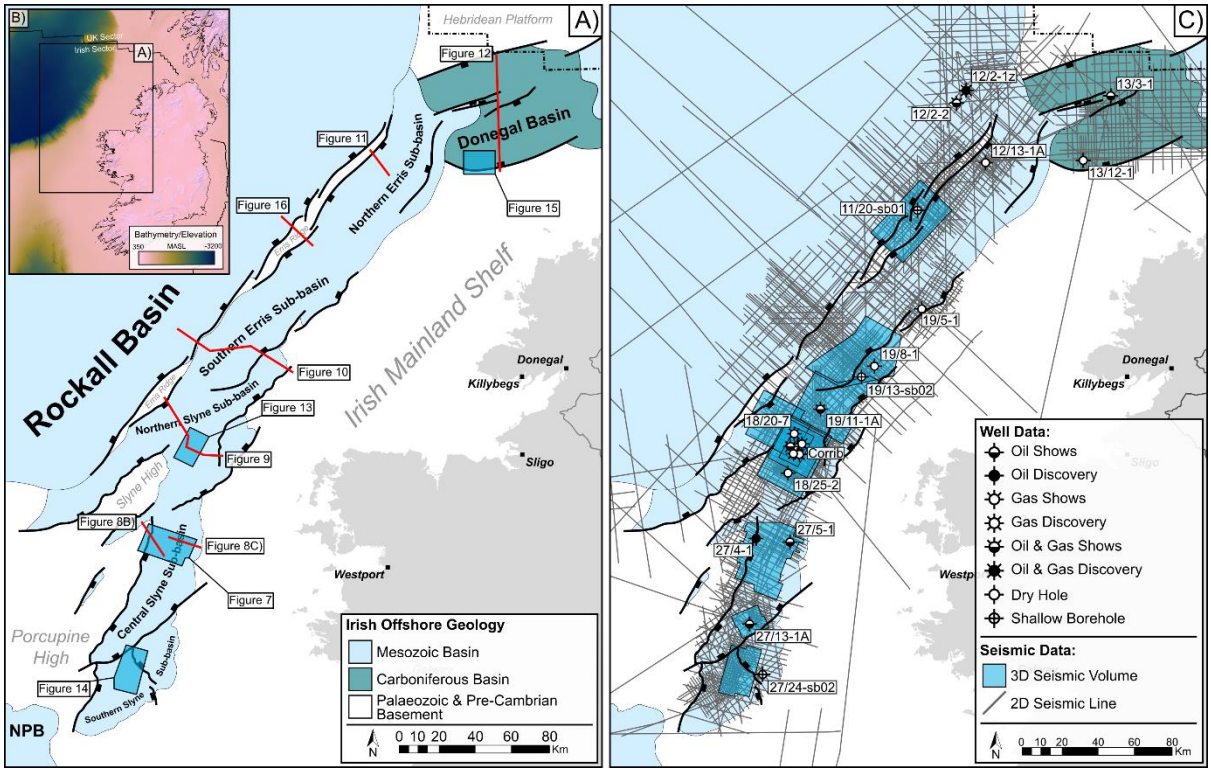

Figure 2: Overview map of the study area. A) Map showing the distribution of basins offshore north-western Ireland. Abbreviations: NPB – North Porcupine Basin. B) Bathymetry around the island of Ireland. Abbreviations: MASL – Metres Above Sea Level. C) Map showing the distribution of borehole and seismic reflection data used in this study.

The geology of the seismic database was constrained using exploration, appraisal, and production wells from the Slyne, Erris and Donegal basins. This includes two wells in the Donegal Basin, two wells in the Erris Basin, and 15 wells in the Slyne Basin. Data from these wells includes wireline logs, formation tops, lithological descriptions, temperature and pressure data from well reports and composite logs, and core data where available. The most recent stratigraphic nomenclature and biostratigraphic ages were used for this study, derived from the recently updated nomenclature for offshore Ireland (Merlin Energy Resources Consortium, 2020).

3.2. Methodology

3.2.1 Regional mapping and structure identification

Geological formations with a significant porous sandstone content represent ideal energy and CO_2 storage candidates. Three sandstone reservoir formations are analysed in the study area, based on their previous identification as hydrocarbon exploration targets (*e.g.* Dancer *et al.*, 2005): Carboniferous, Lower Triassic and Upper Jurassic in age respectively. These reservoir horizons were mapped throughout the study area, to create regional structure maps and understand their distribution. To identify structural closures and measure gross rock volumes, these reservoir horizons were converted from the time domain to the depth domain using a velocity model. This layer model consisted of the Seabed, Base-Cenozoic, Base-Cretaceous, Base Upper Jurassic, Top Triassic, Top Lower Triassic, Top Permian and Base-Permian. An initial velocity (V_0) and k-factor (the change in velocity within that section with increasing depth)

were calculated for each section using well-derived time-depth relationships (Table 1). Due to the variable geology of the study area, some layers were not present in different sub-basins.

Table 1: Values used to depth convert 3D reservoir surfaces. Values derived from well-based velocity data.

Stratigraphic interval	**V_0**	***k***
Water column (surface to seabed)	1500	N/A
Cenozoic	1510	N/A
Cretaceous	2756	N/A
Upper Jurassic	2483	0.50
Lower & Middle Jurassic	3200	0.40
Upper Triassic	4400	0.20
Lower Triassic	4800	0.15
Permian	5000	N/A
Carboniferous	5100	0.10

The regional top reservoir maps were then used in a spill-point analysis to identify structural traps throughout the study area (Møll Nilsen *et al.*, 2015). This method uses nodal analysis on all the points which make up a reservoir surface to locate local maxima which represent structural closures and identifies the deepest spill point on each closure. Depth converted reservoir surfaces were resampled to 250 m by 250 m grids to improve computation time. Polygons representing these identified structural closures were then overlayed on the higher resolution depth converted surfaces to ensure the closure was valid on the more detailed surfaces. These higher resolution surfaces were then used for calculating gross rock volumes.

3.2.2. Calculating storage potential

The potential storage capacity of a structural trap can be calculated as Gas In Place (GIP) using the equation below:

$$GIP = \mathrm{G}RV \times NtG \times \Phi \times S_g \times \rho_g$$

Where GRV (m^3) is the gross-rock volume, NtG is the net-to-gross ratio of reservoir to non-reservoir rock, ϕ is the depth-dependant porosity (*i.e.* fraction of the rock made up of void space), S_g is the maximum gas saturation. This represents the total pore space within a structural closure which can be occupied. This can then be multiplied by the density (ρ_g) of the gases at reservoir conditions to understand how much of each gas (*i.e.* CO_2 and H_2) can be stored in these structures. Values for CO_2 capacity were presented in million tonnes while H_2 values were multiplied by the higher heat capacity of hydrogen (39.4 KWh/kg or TWh/million tonnes) to better understand its grid contribution as an energy storage medium.

A final consideration for injected gas that is to be returned to the surface (*i.e.* H_2) is the requirement for a certain volume of gas to be left in the reservoir to maintain a suitable pressure to support efficient production (termed 'cushion gas'). Therefore, only a portion of the calculated volume in any prospective storage site will constitute gas that can be stored and withdrawn economically. The percentage of the storage volume which will be required to act as cushion gas will vary depending on the initial pressure of individual structures but will likely be between 40-60% of the total volume of a structure (McVay & Spivey, 2001; Klempa

et al., 2019). Therefore, the effective storage capacity of a candidate storage site (commonly termed the 'working gas volume') can be calculated by multiplying the GIP by this percentage.

3.2.3. Gross rock volume (GRV)

Gross rock volume is determined by calculating the volume between the top and base reservoir above the shallowest spill point on that structure. Volumes were calculated between the top and base depth-converted regional reservoir surfaces down to the shallowest spill point for that structural closure. If the base reservoir surface was above the spill point contour, the volume of non-reservoir rock below the base of the reservoir, but above the structural spill point, was subtracted from the GRV.

3.2.4. Net-to-gross (NtG)

The ratio of the gross storage formation that is made up of reservoir-grade rock is termed the net-to-gross (NtG). The NtG of each of the three storage formations evaluated in this study was calculated in each well using a Vshale curve derived from the gamma logs (Asquith *et al.*, 2004). The Vshale curves were then compared with cuttings and core descriptions included in well completion reports and composite logs to ensure that suitable sand and shale cut-offs were defined for each storage play. The NtG values from each well were then extrapolated across the study area to produce predictive NtG maps for each of the storage plays. Due to the sparse point data (typically 10s of kilometres between wells), ordinary kriging was used to interpolate between data points.

3.2.5. Porosity (ϕ)

Porosity data for each of the key storage formations is relatively limited given the few wells drilled in the study area. This data is primarily derived from core and core plug analysis reports included with well completion reports. In data poor areas, like underexplored sedimentary basins, predictive tools can be used to supplement what data does exist. Porosity decreases with increasing burial depth primarily due to mechanical compaction. Empirical compaction curves have been developed for several different regions and lithologies which describe the change in porosity with depth, and can be applied to the reservoir formations on the Irish Atlantic margin. Sclater & Christie (1980) demonstrated that porosity at depth (ϕ_z) can be estimated using the equation below:

$$\phi_z = \phi_0(e^{-cz})$$

Where ϕ_0 is the porosity at the surface, c is the porosity-depth coefficient and z is depth. Due to the geology of the sedimentary basins analysed in this study, this standard equation was modified to account for severe uplift and erosion that have impacted the reservoir formations. This is described in more detail in the storage play characterisation section.

3.2.6. Gas saturation (S_g)

Not all existing formation water can be displaced when gas is injected into a water-saturated porous subsurface reservoir. This is caused by the relative permeabilities of different fluid components (*e.g.* water and CO_2 or water and H_2). Therefore, only a percentage of the total

pore space will be occupied by the injected gas. Several laboratory studies have been carried out in recent years to investigate the relative permeability and theoretical range of gas-saturations for CO_2 and H_2 stored in subsurface sandstone reservoirs (*e.g.* Krevor *et al.*, 2012; Yekta *et al.*, 2018; Hashemi *et al.*, 2021; Rezaei *et al.*, 2022; Thiyagarajan *et al.*, 2022) which indicate a gas saturation range of 0.2 to 0.65. These values will provide upper and lower limits for gas saturation values during volume estimation.

3.2.7. Gas density (ρ_g)

The density of a gas changes with temperature and pressure, both of which increase with increasing depth beneath the earth's surface. These densities were calculated using correlation tables which are based on equations of states for individual gases (*e.g.* Span and Wagner, 1996). Correlations from Lindstrom & Mallard (2022) were used in this study.

Predictive pressure and temperature values for calculating gas densities at reservoir depths were generated using data from exploration wells in the study area. Plotting corrected temperature readings for wells throughout the study area indicate a regional geothermal gradient of 31 °C/km (Fig. 3A). Pressure data is only available for wells in the Slyne Basin, where most wells have encountered a near-hydrostatic pressure gradient of 0.1 Bar/m or 10,000 Pa/m throughout the drilled section (Fig. 3B), including those with breached oil accumulations (*e.g.* the Upper Jurassic reservoirs in the 18/20-1, 27/5-1 and 27/13-1A wells). While no pressure information is available from wells in the Erris or Donegal basins, no indicators of overpressure were encountered in any of the wells drilled in those basins. Therefore, a hydrostatic pressure gradient can be used to reasonably predict pressure changes with depth in these basins.

The main exception is the Lower Triassic reservoir section in the Corrib gas field which is modestly overpressured by c. 45 Bar relative to the regional hydrostatic gradient (Fig. 3C). This may be caused by the overlying Upper Triassic salt preserving higher pressure during exhumation (Corcoran & Doré, 2002). No pressure information is available for the two other structures which encountered the same Lower Triassic reservoir overlain by Upper Triassic salt (wells 18/20-7 and 19/11-1A), although log-derived pressure estimations from the 19/11-1A well suggests it encountered a similarly overpressured reservoir to the Corrib aquifer in the Lower Triassic reservoir (Statoil, 2004). In wells where the Upper Triassic seal is composed of mudstone rather than salt (*e.g.* wells 19/8-1 and 27/5-1), the Lower Triassic reservoir is normally pressured (Enterprise, 1996a; StatoilHydro, 2009).

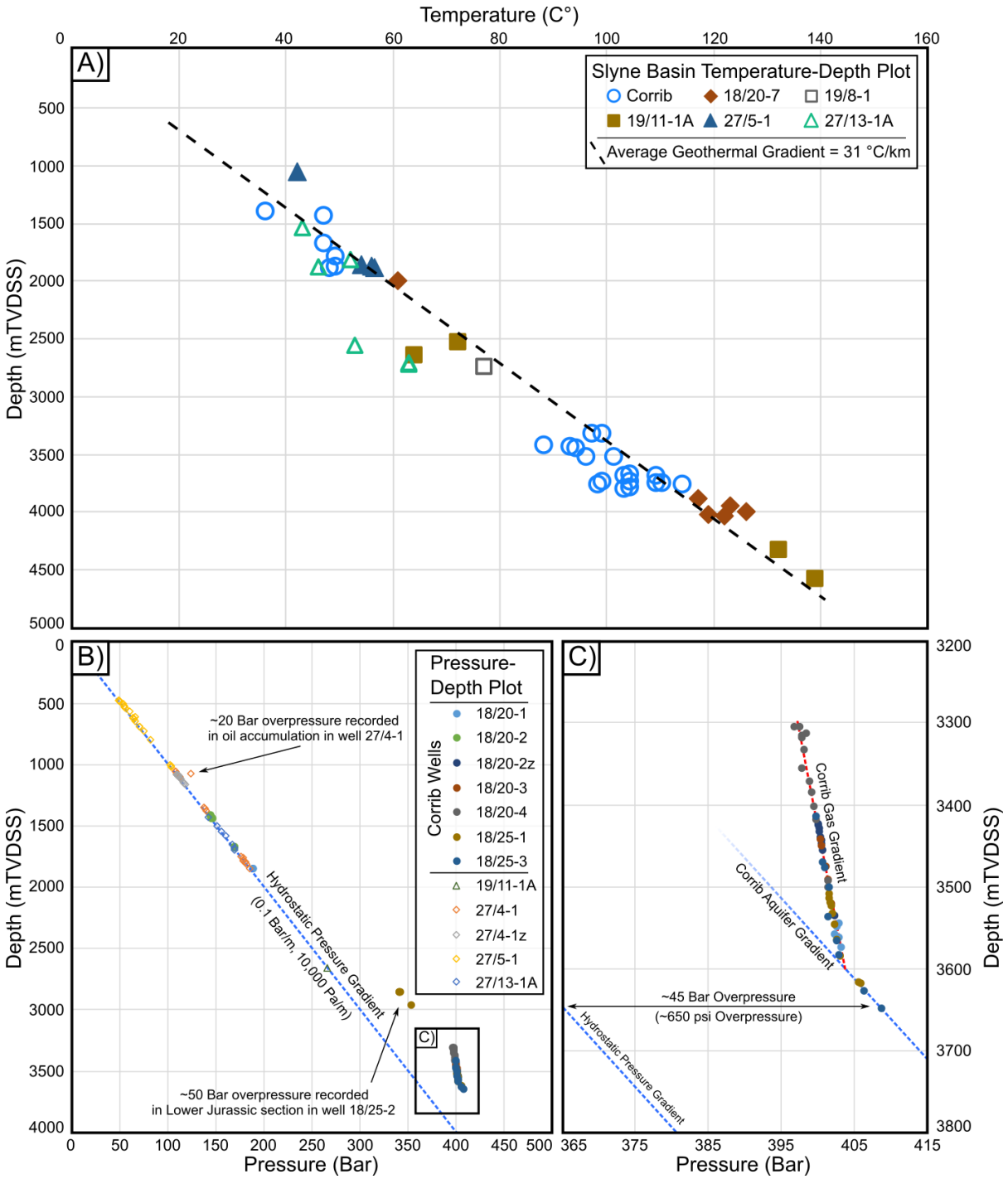

Figure 3: A) Temperature-depth plot for corrected down-hole temperature measurements from the Slyne Basin. B) Pressure-depth plot for all wells in the Slyne Basin. C) Pressure-depth plot for all data from the Lower Triassic section in the Corrib gas field.

4. Geological Setting

The Slyne, Erris and Donegal basins, located offshore north-western Ireland, have been the subject of intermittent hydrocarbon exploration and development for over 50 years (Trueblood, 1992; Scotchman & Thomas, 1995; Shannon & Naylor, 1998; Scotchman *et al.*, 2018). They are a group of broadly contiguous basins located 30-60 kilometres off the north-western coast of Ireland in water depths of 150-3000m (Fig. 2). The basins are elongate and fault-bound, bordered by the crystalline rocks of the Irish Mainland Shelf to the east and the Erris Ridge

and Porcupine High to the west, and belong to a framework of basins of various ages and structural styles which stretch across the Irish Atlantic margin (Fig. 2).

4.1. Tectonostratigraphic evolution

The geology of the study area is a product of a complex geological evolution extending from the Carboniferous to the present day (Chapman *et al.*, 1999; Dancer *et al.*, 1999; O'Sullivan *et al.*, 2022). The oldest rocks investigated in this study are Carboniferous strata deposited in several fault-bound basins which formed during back-arc extension as the Rheic Ocean was subducted beneath the Laurentian continent (Woodcock & Strachan, 2012). These include a predominantly marine Mississippian sequence of limestones, sandstones and mudstones overlain by a terrestrial Pennsylvanian sequence of mudstones, sandstones and layers of coal (Fig. 4; Tate & Dobson, 1989). These Carboniferous basins were locally inverted by compressional forces associated with the Variscan Orogeny (Worthington & Walsh, 2011). Alongside local inversion, regional uplift and erosion created the Variscan Unconformity.

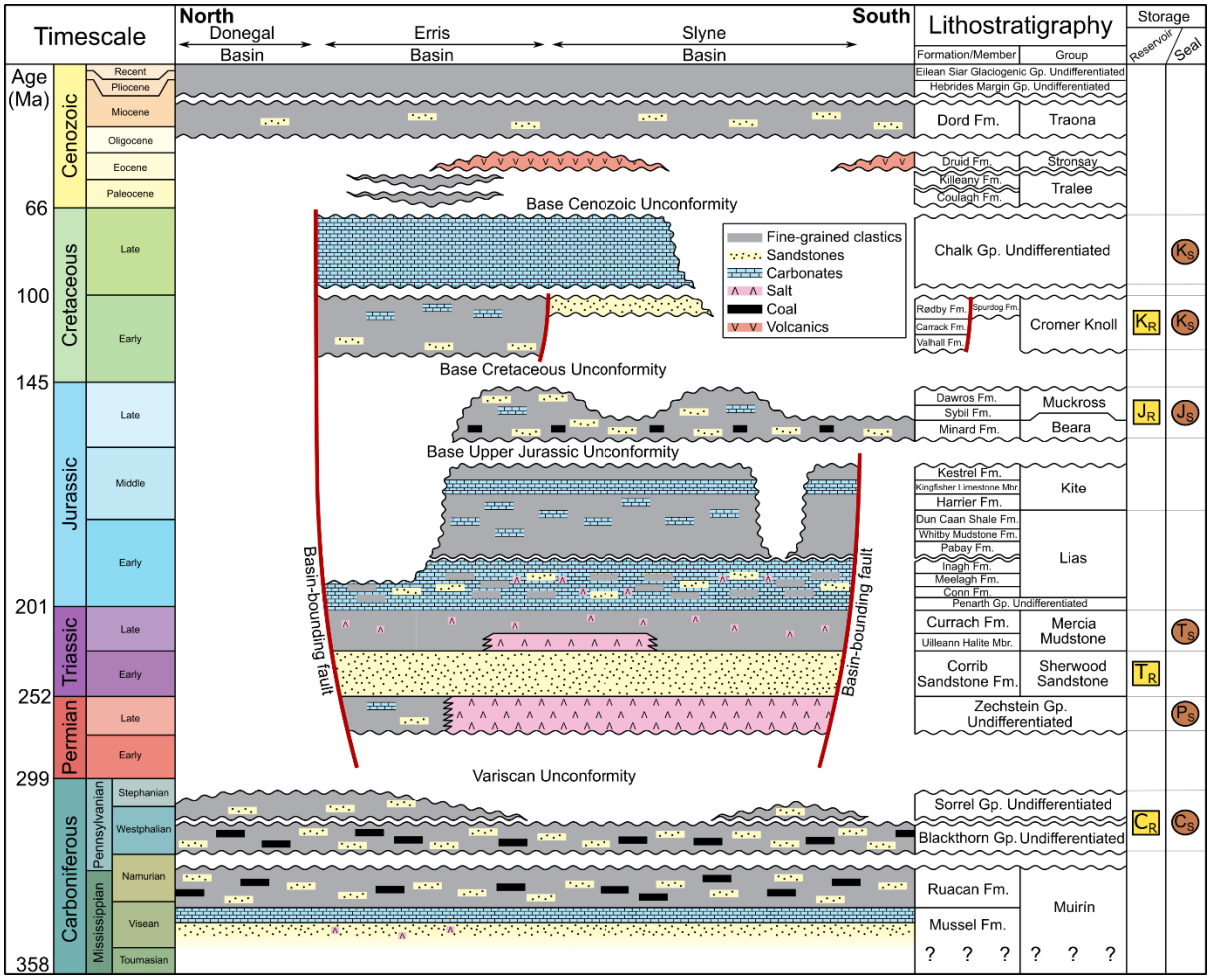

Figure 4: Stratigraphic column for the Slyne, Erris and Donegal basins. The key storage plays are highlighted. The stratigraphic nomenclature is adapted from Merlin Energy Resources Consortium, 2020.

Post-orogenic extension began in the Late Permian, accompanied by the formation of several hundred metres of salt in the hanging walls of active faults alongside thin carbonate and clastic deposits on intrabasinal highs (Doré *et al.*, 1999; O'Sullivan *et al.*, 2021). This was followed by a period of tectonic quiescence during the Early and Middle Triassic, with the development

of a braided river system in an arid environment throughout the study area (Dancer *et al.*, 2005). This was overlain by red mudstones deposited in sabkha and playa lake environments, and locally a second layer of salt, representing an ephemeral marine incursion, during the Late Triassic (Merlin Energy Resources Consortium, 2020). There is also evidence of regional extension and halokinesis initiating during the Late Triassic period (O'Sullivan & Childs, 2021).

A second period of regional extension occurred during the Early and Middle Jurassic in tandem with a marine transgression. A sequence of marine limestones, mudstones and sandstones was deposited throughout the region, thickening into the hanging walls of active faults (Dancer *et al.*, 1999). Several salt structures formed during the Early to Middle Jurassic, including salt anticlines, rollers and walls (O'Sullivan *et al.*, 2021; O'Sullivan & Childs, 2021). Early and Middle Jurassic extension ceased during the late Middle Jurassic when the region experienced uplift and erosion (Dancer *et al.*, 1999). The exact cause of this uplift and erosion is poorly constrained but may be related to a mantle plume in a similar but less severe manner to the North Sea doming event (Ziegler, 1992).

A third extensional phase began during the Late Jurassic, accompanied by kilometre-scale movement on the basin-bounding faults and the deposition of a thick sequence of fluvio-estuarine mudstones and sandstones throughout the study area (Dancer *et al.*, 1999; O'Sullivan *et al.*, 2022). A second phase of halokinesis occurred in tandem, with new structures being formed and pre-existing structures created in the Early and Middle Jurassic being reactivated and modified (O'Sullivan *et al.*, 2021). A marine transgression occurred towards the end of the Jurassic, with the uppermost Jurassic sediments consisting of marine limestones and mudstones (Merlin Energy Resources Consortium, 2020).

Most of the study area experienced kilometre-scale uplift and erosion during the Early Cretaceous, creating a distinct regional unconformity. This was driven by rifting and hyperextension in the neighbouring Rockall Basin to the northeast (Fig. 2). The Erris Basin is a notable exception and was involved in the extension of the Rockall Basin, with over a kilometre of predominantly marine sediments accumulating in this basin during the Cretaceous (Chapman *et al.*, 1999; O'Sullivan *et al.*, 2022). Several structures underwent subtle modification and reactivation during this period of exhumation, with small reverse and normal movements on faults observed throughout the study area (Corcoran & Mecklenburgh, 2005; O'Sullivan *et al.*, 2022).

The area experienced additional periods of uplift during the Cenozoic, which are variously attributed to the Alpine Orogeny, the development of the Icelandic plume and the onset of ocean crust formation and associated ridge-push in the North Atlantic Ocean (Dancer *et al.*, 1999). The magnitude of uplift was less severe than that experienced in the Early Cretaceous, with a few hundreds of metres of sediment removed (Corcoran & Mecklenburgh, 2005). Several structures underwent further modification and reactivation during the Cenozoic as a result of these post-rift tectonic processes (O'Sullivan et al, 2022). Regional magmatism occurred during the Cenozoic, with the intrusion of igneous sills and dykes throughout the Carboniferous and Mesozoic sediments, and the extrusion of lavas over certain parts of the study area (Dancer *et al.*, 2005; O'Sullivan and Childs, 2021). Following the extrusion of these Cenozoic lavas, marine and glaciogenic mudstones and sandstones were deposited throughout the study area during the Cenozoic.

5. Storage play characterisation

Each of the reservoir units is described in terms of a 'storage play' in a similar manner to a 'petroleum play' used in hydrocarbon exploration. The methodologies used are similar to the description of petroleum plays offshore Ireland (*e.g.* Trueblood, 1992; Spencer and MacTiernan, 2001). In a petroleum play, these components include the reservoir, seal, and source rocks alongside a suitable trapping structure and migration pathways for hydrocarbons. Certain components which are required in the petroleum play (*e.g.* the source rock and migration route from source to reservoir) are irrelevant for subsurface gas storage and so are not considered here. Similar concepts have been applied to pure hydrogen storage and termed 'hydrogen plays' (*sensu* Heinemann *et al.*, 2018). Here we expand on this to describe subsurface 'storage plays' which can be used to store a variety of gases including CO_2 and H_2. To achieve this, the stratigraphic nomenclature, depositional environment, regional distribution and reservoir properties including net-to-gross and porosity are described for each of the three main storage plays considered in this study. Some additional storage plays which are more poorly constrained are also discussed.

5.1. Carboniferous storage play (C_R)

The Carboniferous is one of the most poorly understood sedimentary sections within the study area. Being one of the deepest proven sedimentary sections in the area, it was often considered the 'economic basement' at the bottom of most hydrocarbon exploration wells in the region, with only the upper few 10s of metres being penetrated and described. It is also typically characterised by low-amplitude reflectors on seismic data, making regional mapping of distinct markers within the Carboniferous section rather difficult.

The most extensive Carboniferous section was encountered in the 19/5-1 well in the southern Erris Basin. This well encountered 1679 metres of Carboniferous sediment, which can be broadly subdivided into three sections (Fig. 5A). The youngest of these are the Pennsylvanian Sorrel and Blackthorn Groups, which were deposited in a predominantly coastal, deltaic and swampy environment. This section is underlain by the Muirín Group, which is subdivided into the Ruacan and Mussel formations. The Ruacan Formation was deposited in shallow marine and continental settings, while the Mussel Formation was deposited primarily in a continental environment (Merlin Energy Resources Consortium, 2020). The Ruacan and Mussel formations have only been encountered in the 19/5-1 well, while other wells which penetrate the Carboniferous terminate within the Blackthorn Group (Fig. 4). Seismic data, particularly in the Donegal Basin, indicate a thick undrilled sedimentary sequence beneath the Blackthorn Group, which may represent Muirín Group sediments. The Carboniferous section is notably absent in the 18/25-2 well in the Slyne Basin (Fig. 5A), where metasediments tentatively dated as Silurian were encountered beneath the Zechstein Group (Enterprise, 2000). This indicates that there are local highs within the study area where Carboniferous sediments are absent.

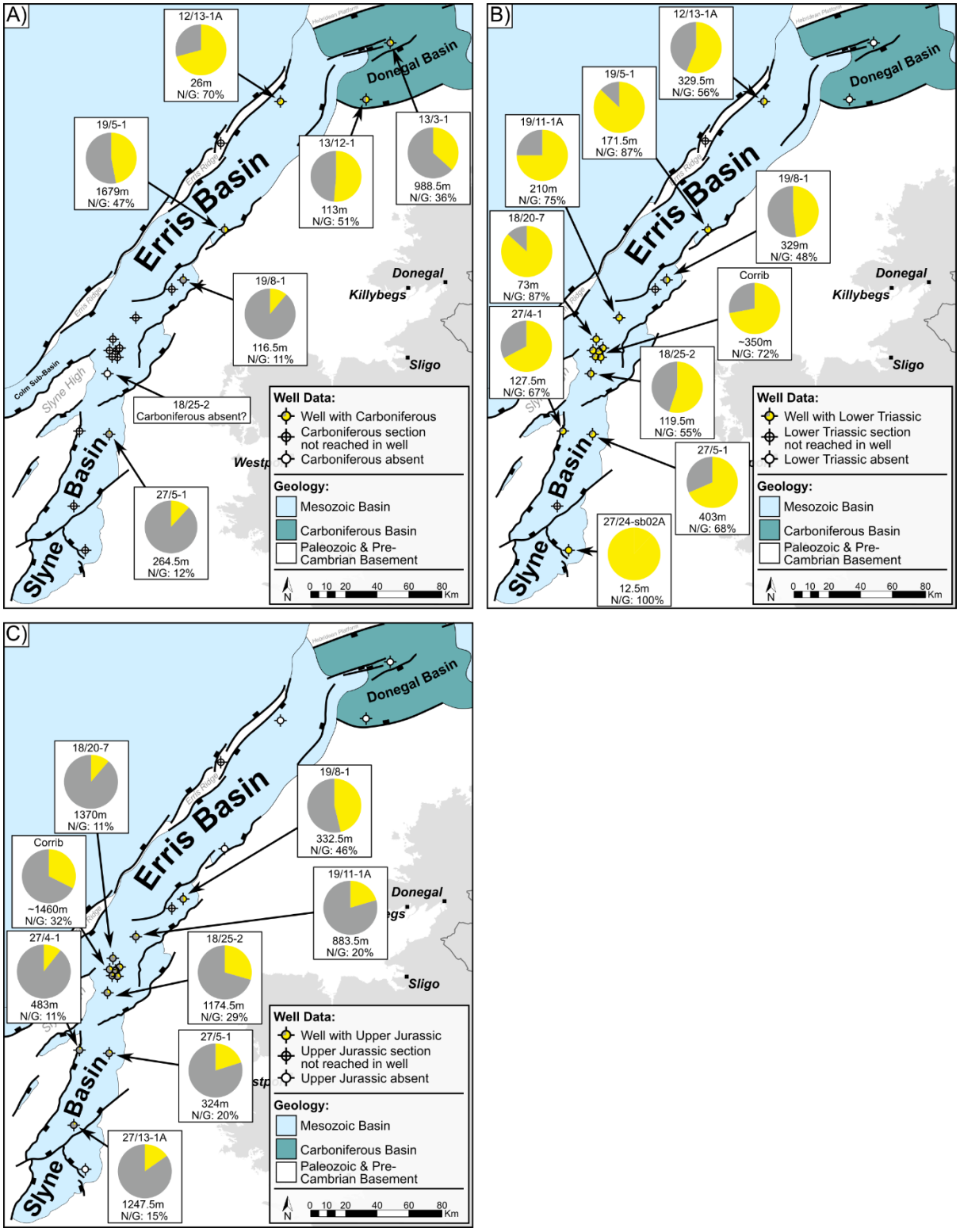

Figure 5: Maps showing the net-to-gross calculated from gamma ray log-based Vshale calculations and lithological descriptions for the A) Carboniferous, B) Lower Triassic and C) Upper Jurassic storage plays in the study area. Reservoir rock is shown in yellow while non-reservoir rock is shown in grey.

The proven reservoir-seal pairs which make up the Carboniferous storage play are the interbedded sandstones and mudstones throughout the Sorrel, Blackthorn and Muirín groups. Within the Sorrel and Blackthorn groups these reservoirs are likely to be relatively narrow and elongate sandstone channels and a predominantly mudstone matrix, due to the deltaic

depositional environment (Tate and Dobson, 1989; Merlin Energy Resources Consortium, 2020), which may limit their lateral extent. Conversely, the sandstones in the Ruacan and Mussel formations likely represent more extensive shallow marine sheet sands and continental aeolian and alluvial fan deposits respectively (Merlin Energy Resources Consortium, 2020). A broad northward increase in the net-to-gross is observed in the relatively sparse Carboniferous well data (Fig. 5A) which may suggest a northern source for the predominantly fluvial Carboniferous reservoir sandstones.

The shallowest Blackthorn Group sandstones in the 13/3-1 well have porosities of 18-34% but this decreased to porosities of 3-5% beneath 500mTVD sub-seabed (Fig. 6, Texaco, 1978). Reasonable reservoir properties were observed in the Blackthorn Group in the 19/5-1 well, with porosities between 9-17% (Fig. 6, Amoco, 1978). The Ruacan Formation in the 19/5-1 well had very limited porosities no higher than 8% (Fig. 6), while the underlying Mussel Formation was described as having no porosity (Amoco, 1978). Both the 12/13-1A and 27/5-1 wells recorded similarly mediocre porosity values around 10% (Fig. 6).

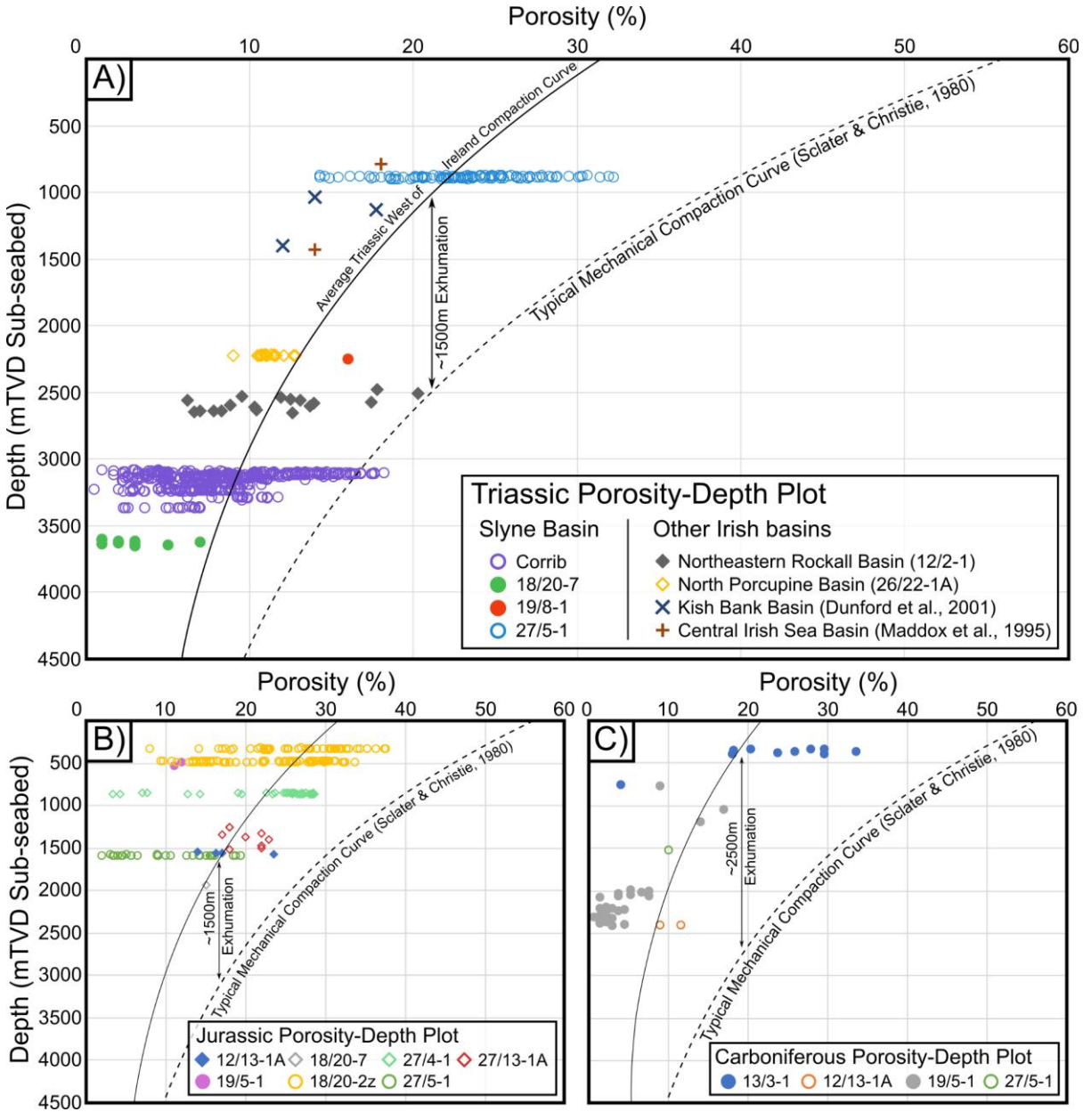

Figure 6: Porosity-depth plots for the three storage plays investigated in this study. A) Lower Triassic, B) Upper Jurassic and C) Carboniferous. Triassic reservoir details from the Kish Bank Basin and Central Irish Sea Basin from Dunford et al. (2001) and Maddox et al. (1995) respectively.

The seal to these Carboniferous sandstones is provided by the mudstones interbedded with the fluvial and deltaic sandstones. These were deposited in the floodplains and swamps surrounding the fluvial and deltaic channels and are likely to be laterally extensive (Merlin Energy Resources Consortium, 2020). No hydrocarbon accumulations have been found in Carboniferous rocks within the study area to indicate if these mudstones provide an adequate seal. The lateral equivalent to this Carboniferous section in the Lough Allen Basin onshore Ireland hosts sub-commercial gas accumulations (Philcox *et al.*, 1992), which suggests the similar mudstones present in the study area could provide an effective seal. Conversely, the presence of gas-charged Cenozoic sediments and seabed pockmarks in the Donegal Basin (Garcia *et al.*, 2014), where the Carboniferous section lies directly beneath the Base-Cenozoic Unconformity, may indicate that cross-fault mudstone-sandstone juxtaposition does not provide an effective seal. Therefore, detailed fault seal analysis will be needed for structural traps which rely on fault offset for closure.

5.2. Lower Triassic storage play (T_R)

The Triassic storage play in the Slyne and Erris basins consists of the Lower Triassic Corrib Sandstone Formation, sealed by the overlying Upper Triassic Currach Formation (Fig. 4). This is the only storage play analysed in this study which also hosts a developed hydrocarbon reservoir (the Corrib gas field). All wells which reached the Lower Triassic section encountered the Corrib Sandstone Formation (Merlin Energy Resources Consortium, 2020).

The Corrib Sandstone Formation was deposited in a broad braided river system with indications of marginal areas of aeolian dune systems and playa lake deposits (Dancer *et al.*, 2005; Merlin Energy Resources Consortium, 2020). This results in very high net-to-gross values greater than 50% observed in the Corrib Sandstone Formation throughout the Slyne and Erris basins (Fig. 5B). Local variations have been noted in the two wells in the Erris Basin, with thin carbonate layers in the 12/13-1A well interpreted as calcrete deposition (Merlin Energy Resources Consortium, 2020), while a distinct volcaniclastic section is recorded in the 19/5-1 well (Amoco, 1978). A shallow borehole on the eastern margin of the Slyne Basin encountered a coarse-grained conglomerate, suggesting more immature and local sediment sourcing towards the basin-margins (Fugro, 1994).

Plotting porosity against depth from various wells in the Slyne and Erris basin supports the kilometre-scale exhumation interpreted by previous authors (*e.g.* Scotchman & Thomas, 1995; Corcoran & Mecklenburgh, 2005; Biancotto *et al.*, 2007). This trend indicates that the expected porosity at a certain depth should be 5-10% less than that predicted by compaction curves from typically shaly-sandstones (*e.g.* Sclater & Christie, 1980). This estimate does not account for the variation in the magnitude of exhumation observed across the study area (*e.g.* O'Sullivan *et al.*, 2022); some exploration wells have encountered Triassic sandstones with better (*e.g.* 19/8-1) and poorer (*e.g.* 18/20-7) porosity values than those predicated by the modified compaction curve (Fig. 6A).

The Corrib Sandstone Formation is sealed by the overlying Upper Triassic Currach Formation. This is primarily composed of red mudstones interbedded with lenses of anhydrite which formed as regional sabkhas and playa lakes during the Late Triassic, and is found throughout the Slyne and Erris basins (Merlin Energy Resources Consortium, 2020). A layer of halite (the Uilleann Halite Member, Fig. 4) is present at the base of the Currach Formation in the Northern Slyne and Southern Erris sub-basins. This has been interpreted to extend into the Central and Southern Slyne sub-basins by Merlin Energy Resources Consortium (2020), but detailed seismic mapping and well interpretation indicate it likely does not extend into these sub-basins (O'Sullivan *et al.*, 2021). This halite layer may represent a more competent seal than the interbedded mudstones and is the seal for the Corrib gas field and the sub-commercial Corrib North gas discovery (well 18/20-7).

5.3. Upper Jurassic storage play (J_R)

Several kilometres of Jurassic sediments are present throughout the Slyne and Erris basins, representing the main syn-rift package in the study area. No Jurassic sediments have been encountered in the Donegal Basin to date (Fig. 5C). The Jurassic can be broadly subdivided into two sections: predominantly marine Lower and Middle Jurassic sections belonging to the Lias and Kite groups respectively, and an Upper Jurassic section consisting of terrestrial, fluvial and estuarine sediments which belong to the Beara and Muckross groups (Fig. 4). A minor regional unconformity separates these two syn-rift packages (Fig. 4).

Several reservoir-seal pairs are present throughout the Jurassic section which consist of interbedded sandstones and mudstones. Typically, the most sand-rich interval is the Upper Jurassic Minard Formation which represents the most prospective Jurassic-aged reservoir section in the study area. The Minard Formation was deposited in a predominantly terrestrial environment, with the reservoirs made up of fluvial channel-fall sandstones and overbank deposits (Merlin Energy Resources Consortium, 2020). The relative distribution of these sandstones can be observed on a root mean square (RMS) amplitude map of a 25 ms TWTT window within the Minard Formation in the Central Slyne Sub-basin (Fig. 7). This map shows a network of fluvial channels flowing broadly southwards towards the Porcupine Basin, as suggested by Tyrrell *et al.* (2007). Within the Central Slyne Sub-basin, channels along the margin of the basin (*i.e.* in the vicinity of the 27/5-1 well) are oriented transverse to the axis of the basin, while the channels in the centre of the basin are parallel to the basin axis, oriented broadly NNE-SSW. This map indicates that while these channelised sandstone bodies represent very high-quality reservoirs, with 20-30% porosity recorded in the core data in the 27/5-1 well (Fig. 6B; Enterprise 1996a), they are not laterally extensive, reducing the total sandstone content (*i.e.* net-to-gross) within any structural trap. This is reflected in the relatively low net-to-gross values of less than 50% observed in all wells which encounter the Minard Formation (Fig. 5C).

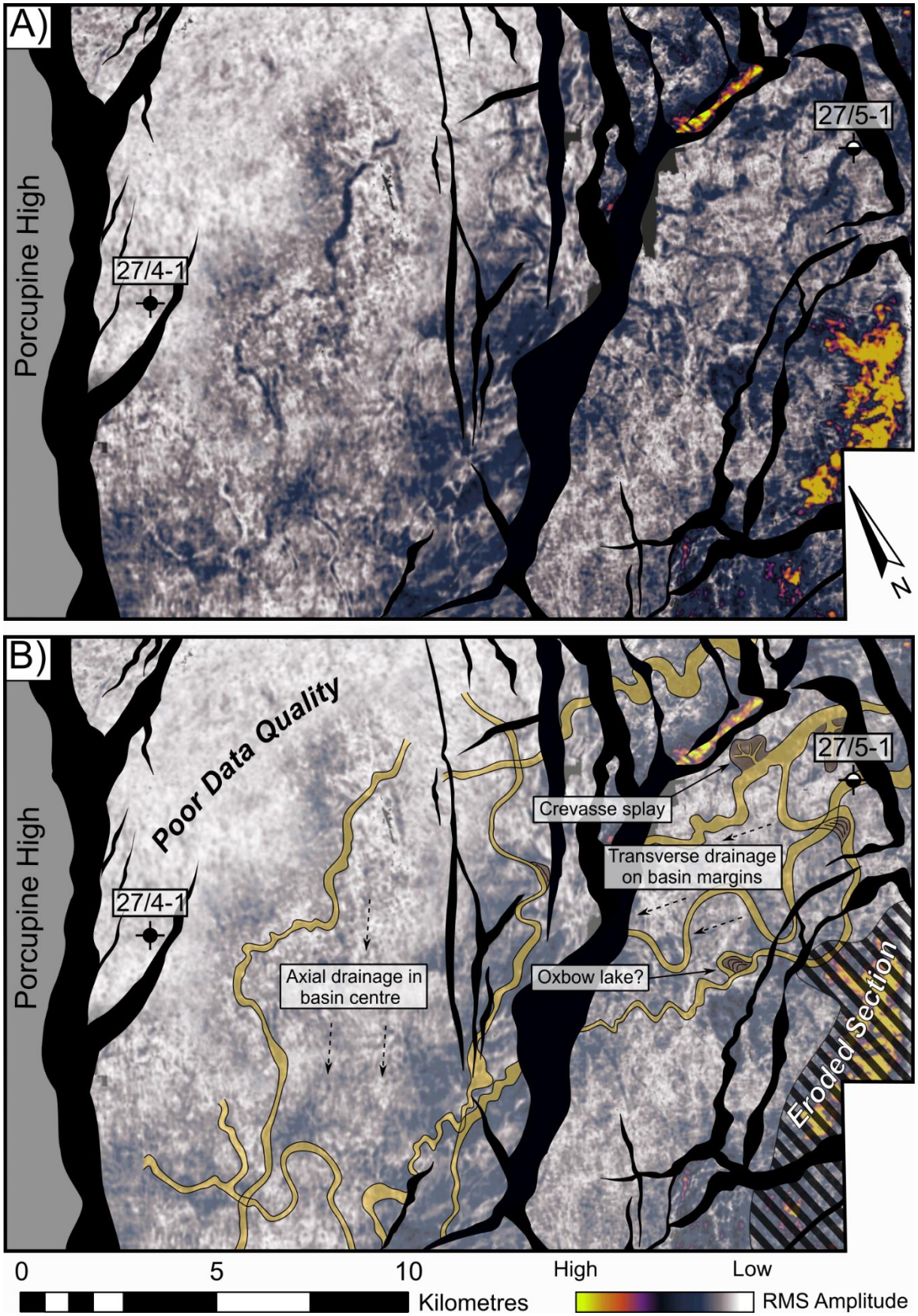

Figure 7: A) Uninterpreted and B) Interpreted RMS amplitude horizon slice in the Upper Jurassic Minard Formation from the Central Slyne Sub-basin illustrating the distribution of fluvial reservoir sandstones in this storage play. Dashed arrows are used to indicate broad paleoflow directions. Fault heave at this horizon is illustrated with black polygons. See Figure 2 for map location.

The interbedded mudstones within the Minard Formation represent continental and lacustrine sediments deposited on the floodplains around the Late Jurassic river systems. These are the principal seals to the interbedded Upper Jurassic sandstones and are likely to be laterally extensive, as suggested by the RMS amplitude map in Figure 7. The integrity of these mudstones as suitable seals does warrant further investigation, as several breached hydrocarbon accumulations have been encountered in previous exploration wells (*e.g.* 18/20-1, 19/11-1A, 27/5-1 and 27/13-1A). The breaching of these paleo-accumulations is attributed to post-charge movement on faults bounding these structural traps (Spencer and MacTiernan 2001).

5.4. Characterising porosity changes with depth in the Slyne, Erris and Donegal Basins:

A key factor in the evolution of the Slyne, Erris and Donegal basins is the significant amount of uplift and erosion which occurred during the Cretaceous and Cenozoic (Chapman *et al.*, 1999; Dancer *et al.*, 1999). Failure to consider the impact of this erosion could lead to overestimation of the porosity and ultimately the capacity of prospective gas storage sites. The magnitude of erosion varies throughout the basin from a few 100s of metres to multiple kilometres (Corcoran & Clayton, 2001; Biancotto *et al.*, 2007). Porosity values recorded from core, core plugs and wireline data for the Carboniferous, Lower Triassic and Upper Jurassic storage plays do not follow the typical mechanical compaction curve of Sclater and Christie (1980) as these sandstones have undergone greater compaction during syn-rift phases prior to being exhumed during post-rift periods in the Cretaceous and Cenozoic (Fig. 6). Shifting the empirical compaction curves vertically by the magnitude of erosion, so that It Aligns with data recorded in the cores and core plugs, corrects for this phenomenon. These modified compaction curves therefore represent a predictive porosity-depth relationship for the reservoir formations on the Irish Atlantic margin which account for uplift and erosion, with the vertical transformation applied to the curve representing the net exhumation magnitude. The spread of porosity values recorded in individual cores and core-plugs also provides a range of expected porosity values at a certain depth.

6. Storage trap types

With the storage plays in the study area established, several potential storage sites are now analysed. Different structural traps are observed throughout the study area, often related to the changing geology between different basins. A key factor in the structural style of individual basins on the Irish Atlantic margin is the presence of the salt layers within the sedimentary section (O'Sullivan *et al.*, 2021). Where salt is present, it will act as a layer of mechanical detachment between the sub- and supra-salt sections and lead to different structures forming either side of the salt (Hudec & Jackson, 2007). Salt can also flow and form salt structures such as salt anticlines and salt rollers (Jackson & Hudec, 2017a; Jackson & Hudec, 2017b). As the presence of salt plays such an important role in the types of structural traps encountered in the different basins, they will be analysed below in three sub-sections:

- The Southern and Central Slyne sub-basins: The Permian Zechstein Group is salt-prone throughout this part of the study area.
- The Northern Slyne and Southern Erris sub-basins: Two layers of salt are present in this part of the study area, the Zechstein Group and the Upper Triassic Uilleann Halite Member.

- The Northern Erris Sub-basin and Donegal Basin: Neither the Triassic or Permian section are salt-prone in the Northern Erris Sub-basin, while both Permian and Mesozoic stratigraphy is largely absent throughout the Donegal Basin.

6.1. Southern and Central Slyne sub-basins

The structural style of the Southern and Central Slyne sub-basins is strongly influenced by the presence of salt within the Zechstein Group. A schematic storage play cartoon is shown in Figure 8. The most common trap types in this part of the study area are horst blocks and tilted fault blocks both above and below the Zechstein Group salt (Fig. 8A). These fault-bound structures were the most common target for hydrocarbon exploration wells in this part of the study area. Of the three exploration wells drilled in the Central Slyne Sub-basin, two targeted fault-bounded horsts and encountered breached oil accumulations (wells 27/5-1 and 27/13-1A). Both structures had evidence of post-charge movement on the bounding faults during the Cenozoic with offset of the Base-Cenozoic Unconformity surface observed (Fig. 8C). This post-charge movement on these faults likely resulted in cross-fault juxtaposition of reservoir sandstones which lead to the loss of hydrocarbon accumulation. Similar movements may yet occur on these structures, which would increase the risk of leakage and loss of any fluids stored in these structures. This places a strong emphasis on detailed fault-seal and fault-stability analysis for any candidate storage sites which rely on a fault for closure.

In addition to the tilted fault blocks, there are also several hanging-wall closures adjacent to the basin-bounding fault along the north-western margin of the basin (Fig. 8B). These are interpreted to have initially formed as forced folds above the incipient basin-bounding faults, before continued slip on these faults breached the folds and resulted in the current structural configuration (Dancer *et al.*, 1999; O'Sullivan *et al.*, 2021). The 27/4-1 well discovered a sub-commercial heavy oil accumulation in Lower Jurassic sandstones in one of these closures (Serica Energy, 2009), suggesting these structures are less prone to reactivation and possible leakage during post-rift tectonic phases.

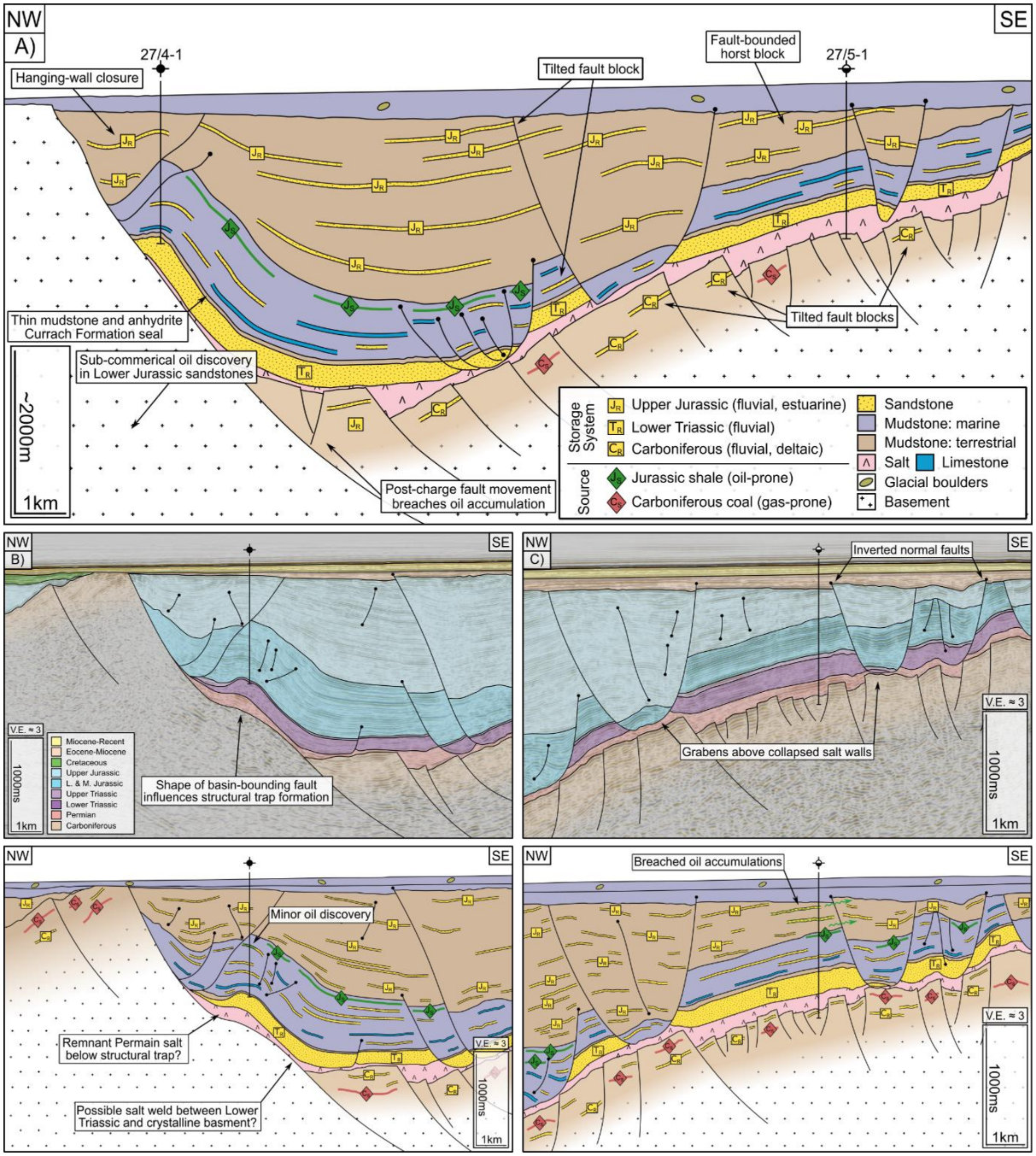

Figure 8: A) Schematic geoseismic section through the Central Slyne Sub-basin highlighting different structural trap types and the distribution of the key storage play components. B) Geoseismic section showing the location of the 27/4-1 'Bandon' oil discovery. C) Geoseismic section showing the impact of Cretaceous and Cenozoic fault movement on the structure hosting the 27/5-1 'Avonmore' breached oil accumulation. See Figure 2 for location.

6.2. Northern Slyne and Southern Erris sub-basins

The presence of two layers of salt in the Northern Slyne Basin (the Permian Zechstein Group and the Upper Triassic Uilleann Halite Member, Fig. 4, 9) results in kinematic interaction between discrete salt structures and the formation of unique structural shapes. The most commonly observed combination is a Zechstein salt anticline and an Uilleann Halite salt wall, with the salt wall oriented parallel to the fold-axis of the salt anticline (Fig. 9). The result of these two composite salt structures are different trap types at different stratigraphic levels: the

formation of the Zechstein salt anticline folds the overlying Corrib Sandstone Formation (the reservoir of the Triassic storage play), forming a four-way dip closure sealed by the overlying Uilleann Halite Member. Above the salt wall formed by this second layer of salt, tilted fault blocks and horsts form in the Lower to Upper Jurassic section (Fig. 9) similar to those observed in the Southern and Central Slyne sub-basins. The presence of the Upper Triassic salt in this part of the study area significantly reduces the risk of top-seal failure for fluids stored in the Lower Triassic storage play relative to other parts of the study area where the Upper Triassic section is composed primarily of red mudstone.

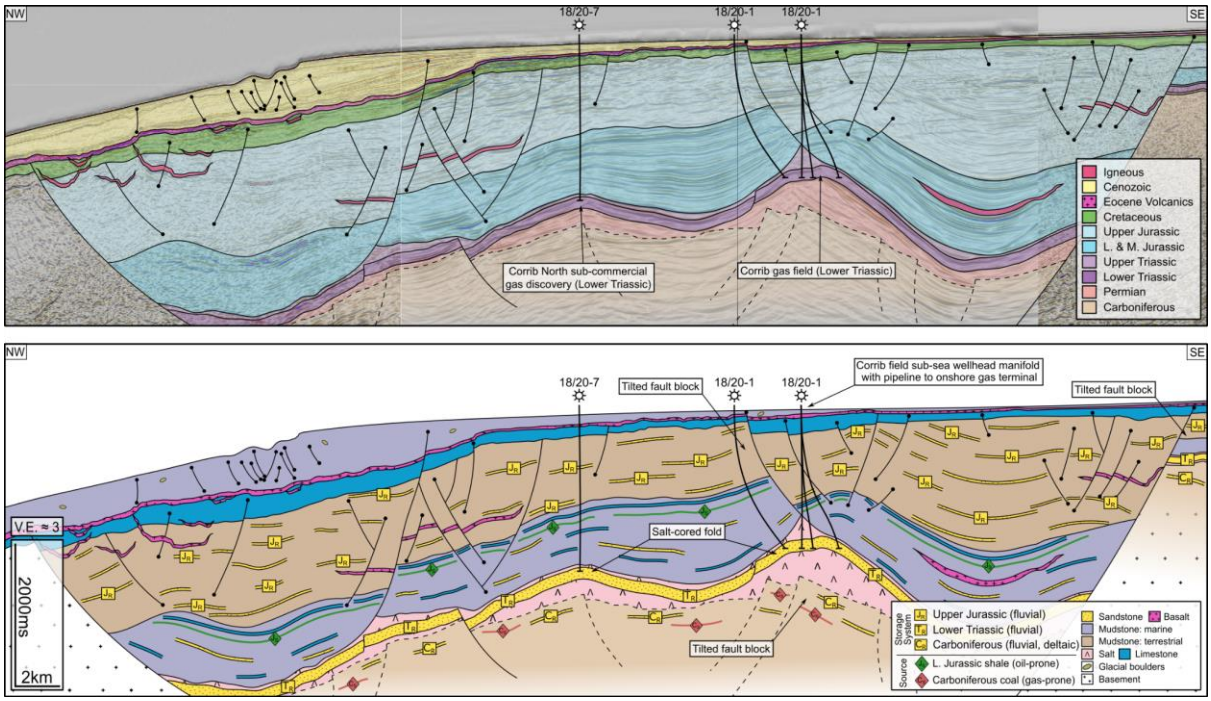

Figure 9: Schematic geoseismic section through the Northern Slyne Sub-basin highlighting different structural trap types and the distribution of the key storage play components. Inset: A) geoseismic section showing the location of the Corrib gas field in the Lower Triassic storage play, and the breached oil accumulation in the Upper Jurassic storage play. See Figure 2 for location.

The stratigraphy of the Southern Erris Sub-basin is more ambiguous than the Northern Slyne Sub-basin due to the lack of historic hydrocarbon exploration in this part of the study area. Nevertheless, previous studies have identified similar structures to those drilled in the Northern Slyne Sub-basin (Fig. 9) including tilted fault blocks and horsts bounded by faults which sole-out in layers of salt (Chapman *et al.*, 1999; O'Sullivan *et al.*, 2021). A schematic geoseismic cross-section of the sub-basin is shown in Figure 10. In the present day the Southern Erris Sub-basin dips steeply towards the northwest as a result of regional thermal subsidence of the neighbouring Rockall Basin. The Southern Erris Sub-basin is also the deepest part of the study, with most of the basin located in water depths in excess of 1000 metres (Fig. 10). Tilted fault blocks are the most common trap type in the Upper Jurassic storage play, with most bounded along their western flanks by westward dipping faults soling out in either the Uilleann Halite Member or Zechstein Group salt layers (Fig. 10). Structural traps in the Lower Triassic storage play are more varied, with some salt-cored folds similar to those found in the Northern Slyne Sub-basin being observed, alongside fault-bound horsts encased in salt (Fig. 10).

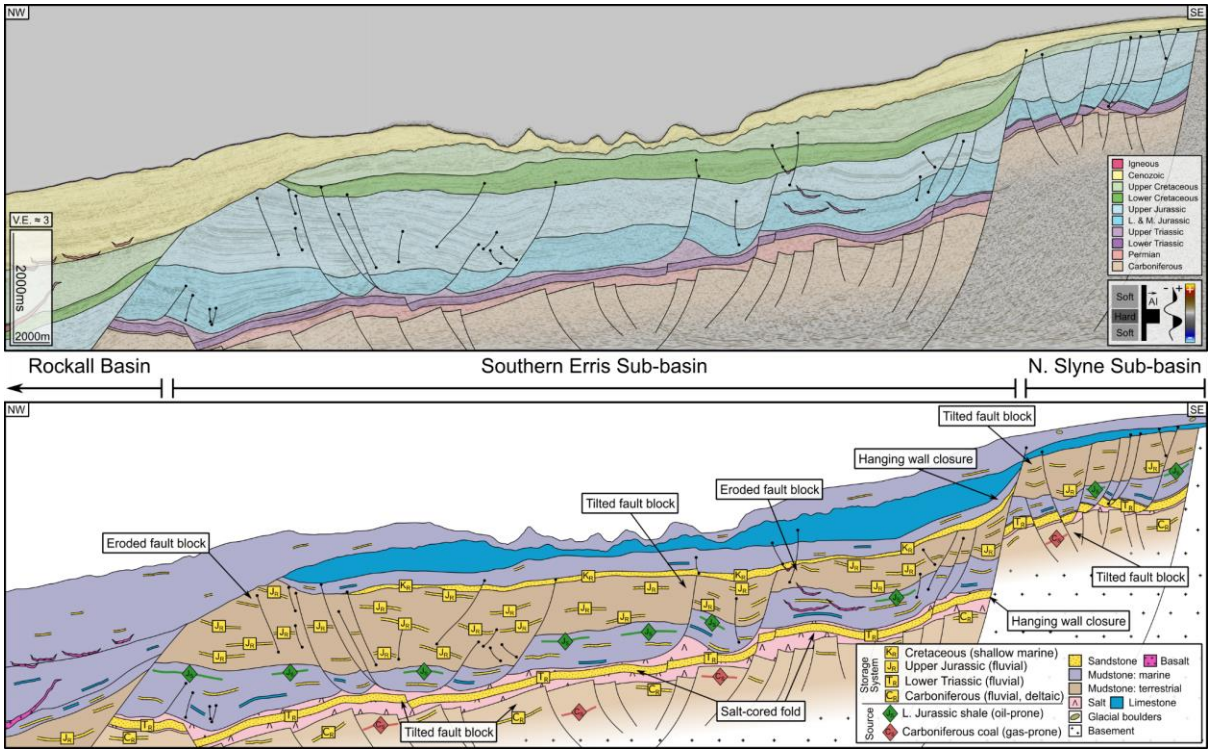

Figure 10: Schematic geoseismic section through the Southern Erris and Northern Slyne sub-basins highlighting different structural trap types and the distribution of the key storage play components. See Figure 2 for location.

6.3. Northern Erris Basin Sub-basin

The structural style in the Northern Erris Sub-basin is noticeably different from its southern neighbours due to the lack of either the Zechstein Group or Uilleann Halite Member salt layers. The sub-basin is characterised by several north-westward-dipping tilted fault blocks covered by a thick Cretaceous and Cenozoic section (Fig. 11). The Northern Erris Sub-basin straddles relatively similar water depths to those in the Southern Erris Sub-basin, with the western margin of the sub-basin being in water depths over 1000 metres.

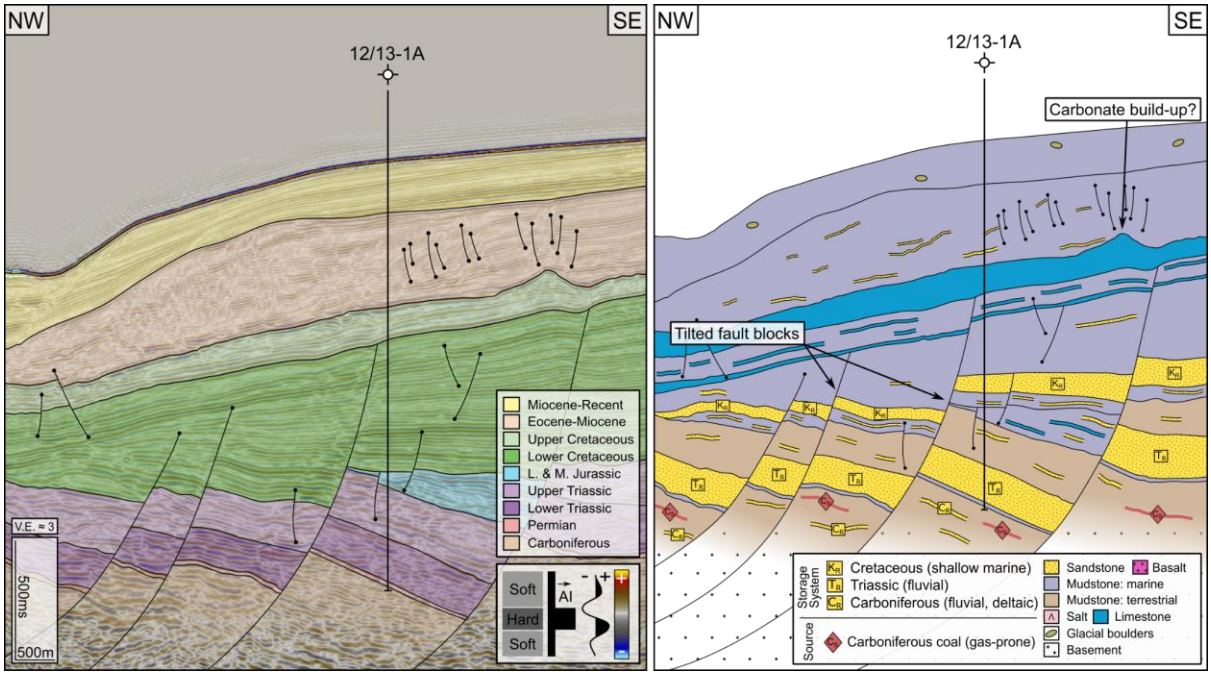

Figure 11: Geoseismic section and schematic play cartoon from the Northern Erris Sub-basin highlighting structural trap types and the distribution of the key storage play components. See Figure 2 for location.

The Upper Jurassic storage play is largely absent in this part of the study area (Fig. 5C, 11), likely due to kilometre-scale uplift and erosion during the Early Cretaceous along the flanks of the Rockall Basin (Chapman *et al.*, 1999; Corcoran & Mecklenburgh, 2005). This leaves the Lower Triassic and Carboniferous storage plays as viable reservoir units in the Northern Erris Sub-basin in primarily fault-bounded structural traps (Fig. 11).

6.4. Donegal Basin

The Donegal Basin is a markedly different basin to both the Slyne and Erris basins. It is predominantly a Carboniferous-aged basin which formed prior to the Variscan Orogeny and was partially inverted by compressional forces associated with that mountain-building event, (Dobson & Whittington, 1992). There is no proven Permian or Mesozoic stratigraphy in this basin (Merlin Energy Resources Consortium, 2020), meaning that both the Lower Triassic and Upper Jurassic storage plays are likely absent across most of this part of the study area (Fig. 5B, 5C).

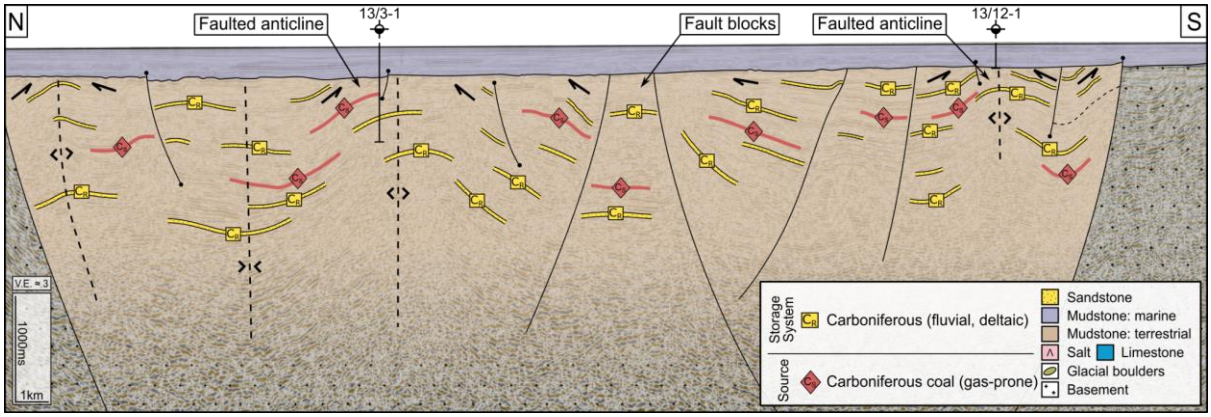

Figure 12: Schematic geoseismic section through the Donegal Basin highlighting different structural trap types and the distribution of the key storage play components. See Figure 2 for location.

The basin is characterised by broad, relatively symmetrical folds with fold axes oriented broadly E-W. which are typically between 10 and 15 km wide and have amplitudes of 1-2 km (Fig. 12). These folds are cut by several normal faults, which may be related to regional post-Variscan extension in either the Permian, Jurassic or Cretaceous. Some of these faults are also observed offsetting the Base-Cenozoic unconformity, indicating relatively recent fault movement similar to the other basins in the study area. Some of these recently active faults have been linked to seafloor seepage features such as pockmarks which suggests these faults represent pathways for hydrocarbon migration to the shallow seabed (Garcia *et al.*, 2014).

The broad folds represent the primary structural trap type in the Donegal Basin which could be used for subsurface storage. Several of these folds are cut by younger normal faults which, as noted above, represent potential leak points for any fluids stored in the Carboniferous sandstone storage play. Folds unaffected by the post-folding normal faulting are present in the Donegal Basin (Fig. 12) and may represent more competent storage sites.

7. Example storage site case studies

With the methodology established and the geology of study area characterised, three potential storage sites are investigated. Each site has different amounts of data available, with first having both high-quality, borehole-constrained 3D seismic data, the second only having 3D seismic reflection data without well control, and the third having only a grid of 2D seismic lines available. Each structure is outlined in detail below:

- The Corrib structure hosts an actively producing gas field in the Lower Triassic storage play. The field is covered by several vintages of 3D seismic data with the most recent being a high-quality ocean-bottom cable survey acquired in 2013. This is tied to data from eight wells. Structural closures are mapped in the Upper Jurassic and Lower Triassic storage plays.
- The Inishmore structure is covered by reasonable quality 3D seismic data. The nearest exploration well (27/13-1A) is located c. 25 kilometres to the north of the structure. Structural closures are mapped in the Upper Jurassic, Lower Triassic and Carboniferous storage plays.
- The Inishbeg structure is covered by a grid of 2D seismic reflection lines with a one-five kilometre spacing. A very shallow exploration well (13/12-1) penetrated the upper 112 metres of the sub-Cenozoic sediments above the structure. The nearest exploration wells of significance (13/3-1 and 12/13-1A) are c. 35 and 45 kilometres to the north and west of the Inishbeg structure respectively. A structural closure is mapped in the Carboniferous storage play.

7.1. Corrib

The Corrib structure hosts the eponymous Corrib gas field in the Northern Slyne Basin. Similarly to the salt-cored fold structures discussed previously, three principal components comprise the structure; a Zechstein Group salt anticline folds the overlying Corrib Sandstone Formation and forms the four-way dip-closure of the reservoir (Dancer *et al.*, 2005). This is overlain by the Uilleann Halite Member forming a narrow salt wall broadly parallel to the fold axis of the Zechstein Group salt anticline (Fig. 13). The Jurassic overburden is deformed by a series of faults related to the growth of the salt structures, with the largest being the Corrib

Fault (O'Sullivan and Childs, 2021), which dips towards the southeast (Fig. 13). The footwall of this fault forms a tilted fault block structural closure. A relatively thin veneer of unconformable Cretaceous and Cenozoic sediments records the complex post-rift evolution of the area (Dancer *et al.*, 2005; O'Sullivan and Childs, 2021).

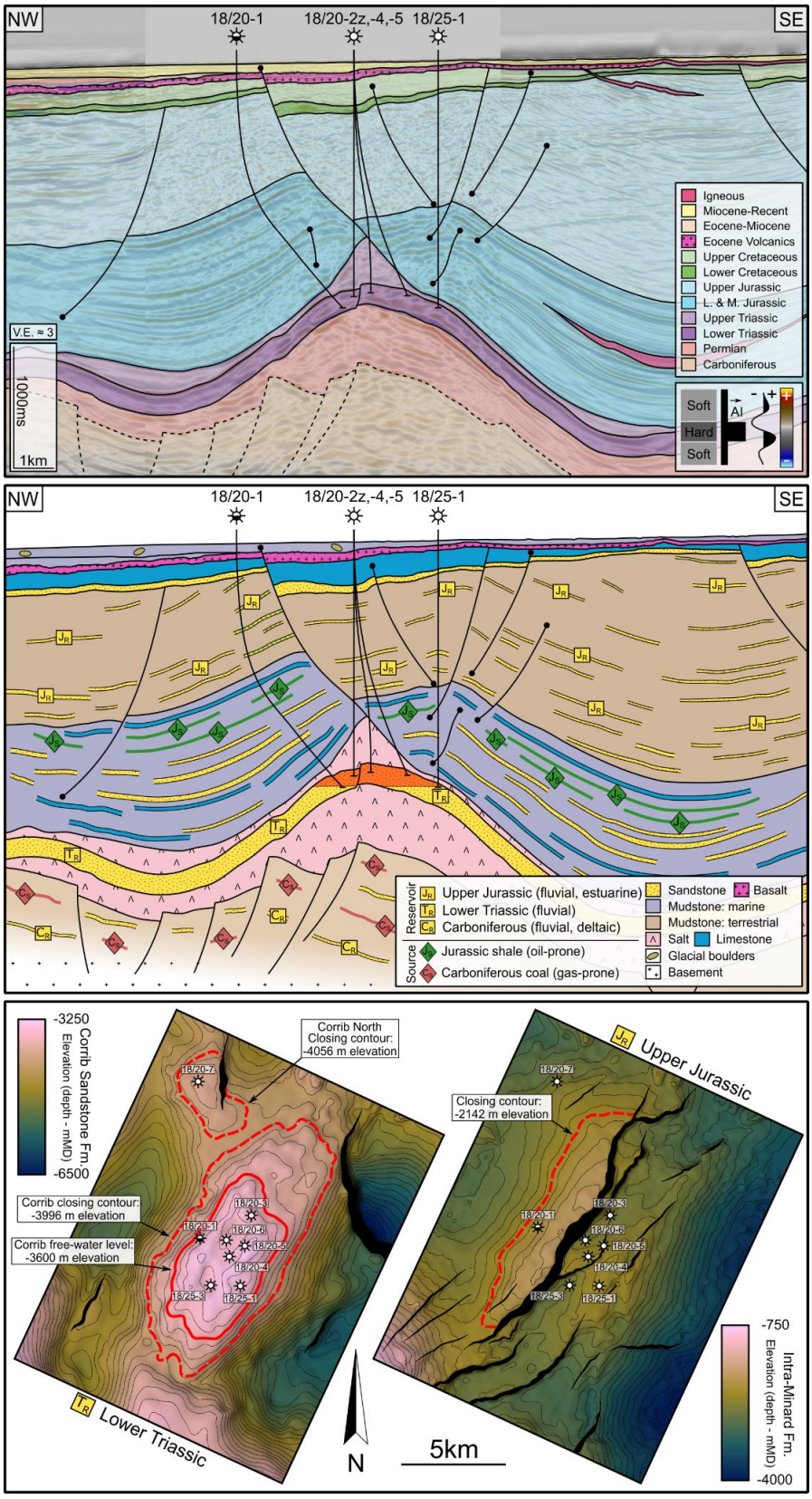

Figure 13: Overview of the Corrib structure. A) Geoseismic section through the Corrib structure. B) Schematic cross-section showing the various storage plays present in the Corrib structure. C) Intra-Upper Jurassic structure map showing the closures mapped in the Upper Jurassic storage play. D) Top Lower Triassic structure map showing the closure mapped in the Lower Triassic storage play. See Figure 2 for map location.

The field was discovered in 1996 with the 18/20-1 well, which encountered breached oil accumulations in the Jurassic tilted fault block followed by the gas accumulation in the Corrib Sandstone Formation (Enterprise, 1996b). The original reserves of the field are c. one trillion cubic feet of gas, which was developed through a subsea tieback to an onshore gas processing plant onshore (Dancer *et al.*, 2005). The Corrib Sandstone reservoir was modestly overpressured prior to production but has likely decreased in pressure since production began in 2015.

Two storage plays are modelled at Corrib: The Lower Triassic storage play, which currently hosts the gas accumulation in the anticlinal closure, and the Upper Jurassic storage play, which contains evidence of a paleo-oil accumulation which has been destroyed, likely by post-charge movement on the fault bounding the tilted block (Enterprise, 1996b). Two spill points were used for the Lower Triassic storage play at Corrib given existing information: the first being located at 3600 mTVDSS matching the gas-water contact which was first encountered during the discovery of the field, and the second at 3996 mTVDSS representing the spill point of the total structural closure. Previous authors have provided several possible explanations for the underfilled nature of the Corrib structure, including a sub-seismic leaking fault or salt weld (Corcoran & Mecklenburgh, 2005) or post-charge modification of the structure (O'Sullivan *et al.*, 2021). In addition to the main Corrib closure, the storage volume of the satellite gas accumulation discovered in the Corrib North structure was also modelled (Fig. 13).

Table 2: Inputs and results for storage assessment in the Corrib and Corrib North structures.

Structure	Corrib Jurassic		Corrib Triassic (Gas)		Corrib Triassic (Full Closure)		Corrib North	
Water depth (m)	355						401	
Top reservoir depth (mTVDSS)	1724		3231		3231		3839	
Base closure depth (mTVDSS)	2142		3600		3996		4056	
Structural relief (m)	417		369		765		217	
Volumetric Input	Maximum	Minimum	Maximum	Minimum	Maximum	Minimum	Maximum	Minimum
GRV (m3)	4.75E+09	3.81E+09	4.61E+09	3.69E+09	1.81E+10	1.45E+10	8.18E+08	6.56E+08
Porosity (%)	31	1	15	1	15	1	13	1
Net-to-gross (%)	46	11	87	48	87	48	87	48
Gas saturation (%)	65	20	65	20	65	20	65	20
CO_2 Density (kg/m^3)	715	703	685	681	685	679	679	677
H_2 Density (kg/m^3)	14.9	12.5	22.4	20.6	23.7	20.6	24.6	23.3
Volumetric Results	**P10**	**P50**	**P90**	**P10**	**P50**	**P90**	**P10**	**P50**	**P90**	**P10**	**P50**	**P90**
CO_2 (Million Tonnes)	136	48	11	119	54	15	497	232	62	14	6	2
H_2 (TWh)	48	17	5	79	32	9	308	147	39	13	6	2

7.2. Inishmore

The Inishmore structure is located in the centre of the Southern Slyne Sub-basin and consists of a tilted fault block above a large salt roller of Zechstein Group halite, oriented NE-SW with the main fault bounding the structure along its south-eastern margin (Fig. 14). The structure has a prominent angular unconformity along its crest at the base of the Upper Jurassic section, indicating that the salt roller had already formed during the Early to Middle Jurassic, likely due

to regional extension, before further salt movement and growth during the Late Jurassic (O'Sullivan *et al.*, 2021). Unlike other structures which have undergone post-rift modification such as the horst block drilled by the 27/5-1 well (Fig. 8C), the faults bounding the Inishmore structure do not offset the Base-Cenozoic Unconformity (Fig. 14), suggesting they may not have been reactivated during the Cenozoic. However, the lack of any Cretaceous sediments to record fault movement during the Cretaceous does not preclude any post-rift movement on the bounding faults (*e.g.* O'Sullivan *et al.*, 2022).

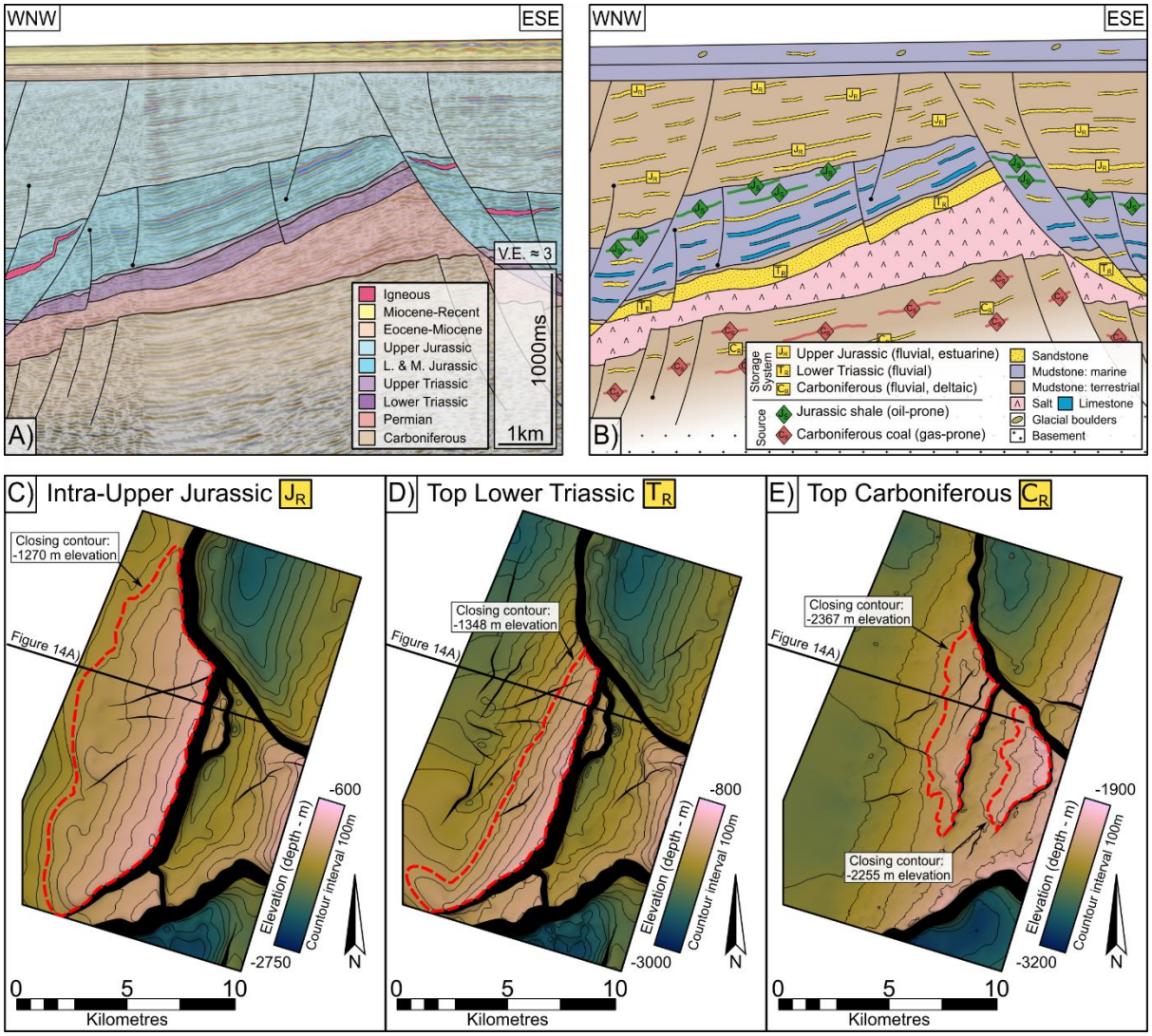

Figure 14: Overview of the Inishmore structure. A) Geoseismic section through the Inishmore structure. B) Schematic cross-section showing the various storage plays present in the Inishmore structure. C) Intra-Upper Jurassic structure map showing the closure mapped in the Upper Jurassic storage play. D) Top Lower Triassic structure map showing the closure mapped in the Lower Triassic storage play. E) Top Carboniferous structure map showing the closures mapped in the Carboniferous storage play. See Figure 2 for map location.

Stacked structural traps are mapped in each storage play in the Inishmore structure; two large closures in the Upper Jurassic and Lower Triassic storage plays are observed bounded by the main fault which soles out in the Zechstein Group halite, while two smaller closures are observed in the Carboniferous storage play (Fig. 14C-E). The Upper Jurassic reservoir is shallower than the 800 metres depth requirement for CO_2 storage but would be suitable for H_2 storage (Fig. 14C), while both the Triassic and Carboniferous reservoirs are deep enough to

be effective for both H_2 and CO_2 storage (Fig. 14D, E). The range of gas volumes for each storage play are presented in Table 3.

Table 3: Inputs and results for storage assessment in the Inishmore structure.

Structure	Inishmore Jurassic			Inishmore Triassic			Inishmore Carboniferous 1			Inishmore Carboniferous 2		
Water depth (m)	151											
Top reservoir depth (mTVDSS)	657			818			2031			2177		
Base closure depth (mTVDSS)	1270			1348			2255			2367		
Structural relief (m)	613			530			224			190		
Volumetric Input	Maximum	Minimum		Maximum	Minimum		Maximum	Minimum		Maximum	Minimum	
GRV (m3)	1.68E+10	1.35E+10		5.66E+09	4.54E+09		6.91E+08	5.54E+08		1.25E+09	9.99E+08	
Porosity (%)	39	4		29	9		20	1		19	1	
Net-to-gross (%)	46	11		87	48		71	11		71	11	
Gas saturation (%)	65	20		65	20		65	20		65	20	
CO_2 Density (kg/m^3)	N/A	N/A		770	733		706	699		703	697	
H_2 Density (kg/m^3)	9.9	4.9		10.6	6.4		16.1	14.3		16.9	15.5	
Volumetric Results	**P10**	**P50**	**P90**	**P10**	**P50**	**P90**	**P10**	**P50**	**P90**	**P10**	**P50**	**P90**
CO_2 (Million Tonnes)	N/A	N/A	N/A	310	174	92	16	7	2	29	11	3
H_2 (TWh)	125	47	16	84	45	24	8	2	1	13	4	1

The influence of salt tectonics on storage volumes can be readily observed in the Inishmore structure; the two phases of fault movement and salt roller growth which affected the Triassic reservoir have resulted in a more steeply dipping top reservoir surface and a smaller closure area (Fig. 14) and smaller storage volume (Table 3) while the overlying Upper Jurassic reservoir has only undergone one episode of tilting during the regional extension in the Late Jurassic, resulting in a shallower dip and greater closure volume.

7.3. Inishbeg

The Inishbeg structure is an anticline located on the southern margin of the Donegal Basin (Fig. 2A). It was previously a hydrocarbon exploration target, with a prognosed Mesozoic section forming a similar structural trap as the Corrib gas field. It was partially tested in 2006 with the 13/12-1 well, which was terminated after only seven days of drilling when it was confirmed that the Mesozoic section was absent in this area and Carboniferous sediments were present directly beneath the Base-Cenozoic Unconformity (Lundin, 2006). Nevertheless, the well only penetrated the upper 100 metres of the Carboniferous section, and the four-way dip closure imaged on seismic data was not fully tested. This same structure is assessed here for its subsurface storage potential and showcases the potential of the Carboniferous storage play in the Donegal Basin (Fig. 15).

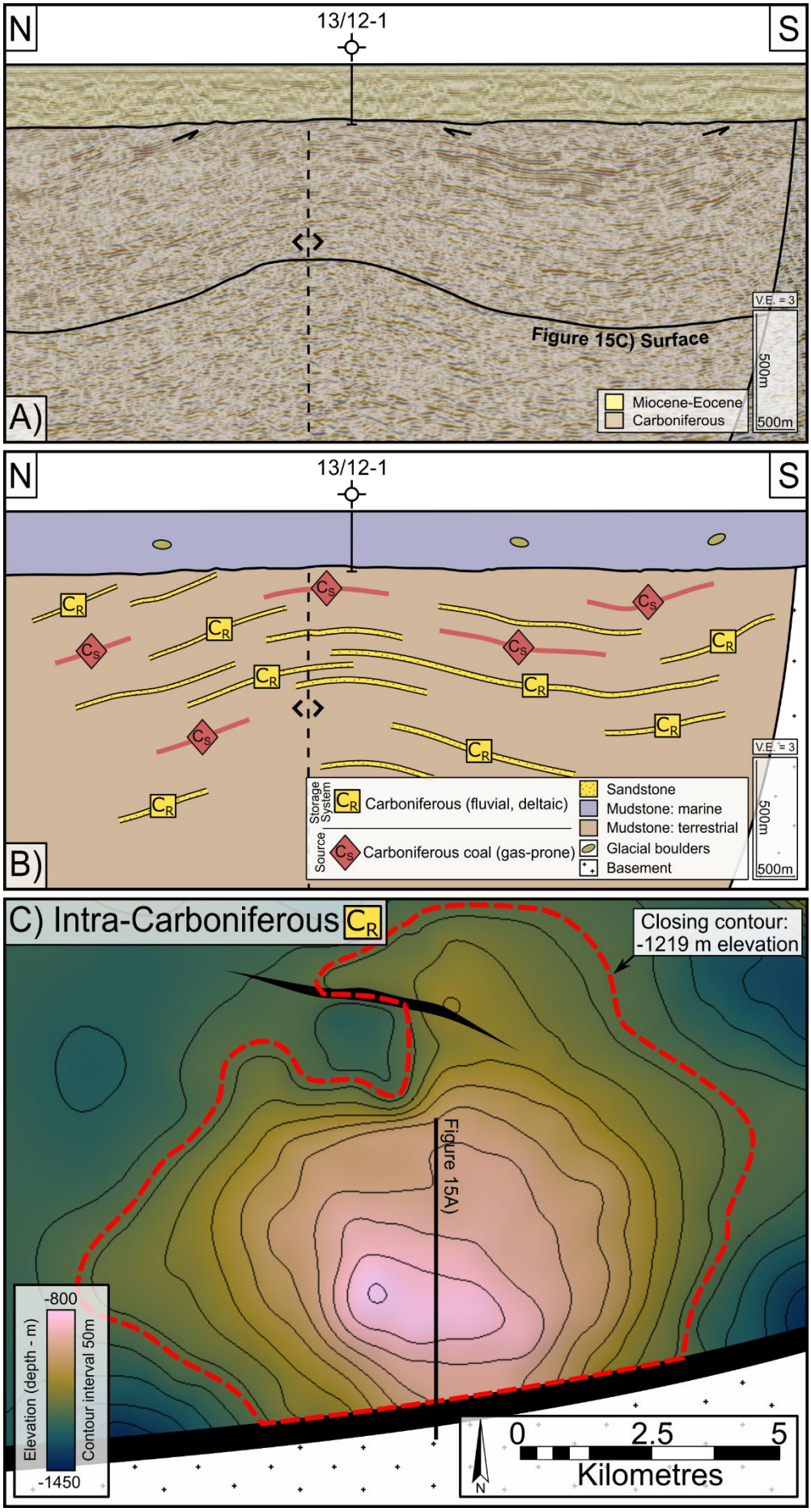
N
13/12-1
S
A)
Figure 15C) Surface
V.E. = 3
500m
500m
Miocene-Eocene
Carboniferous
B)
Storage System
Source
Carboniferous (fluvial, deltaic)
Carboniferous coal (gas-prone)
Sandstone
Mudstone: marine
Mudstone: terrestrial
Glacial bounders
Basement
C) Intra-Carboniferous
Closing contour:
-1219 m elevation
Figure 15A)
Elevation (depth - m)
-800
-1450
Contour interval 50m
0
2.5
5
Kilometres
N

Figure 15: Overview of the Inishbeg structure. A) Geoseismic section through the Inishbeg structure. B) Schematic cross-section showing the Carboniferous storage play present in the Inishbeg structure. C) Intra-Carboniferous structure map showing the closure mapped in the Carboniferous storage play. See Figure 2 for map location.

As the seismic character of the Carboniferous section is relatively homogeneous and lacks distinct seismic markers, a representative reservoir surface was mapped with a structural high at 800m depth (Fig. 15). This reflector was chosen to give a reasonable volumetric estimate considering the typical depth of circa 800m where CO_2 enters a supercritical state. The trap is partially closed by a major fault which forms the southern boundary of the Donegal Basin (Fig. 15). Along-strike this fault has been reactivated during the Cenozoic with a reverse sense of motion (Fig. 12) which emphasises the role of detailed fault analysis in further investigation of these structures.

Table 4: Inputs and results for storage assessment in the Inishbeg structure.

Structure	Inishbeg Carboniferous		
Water depth (m)	97		
Top reservoir depth (mTVDSS)	800		
Base closure depth (mTVDSS)	1219		
Structural relief (m)	419		
Volumetric Input	**Maximum**	**Minimum**	
GRV (m3)	1.41E+10	1.13E+10	
Porosity (%)	33	3	
Net-to-gross (%)	71	11	
Gas saturation (%)	65	20	
CO_2 Density (kg/m^3)	770	739	
H_2 Density (kg/m^3)	9.3	6.4	
Volumetric Results	**P10**	**P50**	**P90**
CO_2 (Million Tonnes)	566	242	60
H_2 (TWh)	140	50	12

The three structures investigated here can hold c. 774 million tonnes of CO_2 and H_2 gas with an energy content of c. 350 TWh (achieved by summing the P50 values for each individual storage play). This demonstrates the considerable storage potential in Ireland's sedimentary basins with regards to the annual emissions (61.8 million tonnes CO_2 equivalent *sensu* SEAI, 2022) and monthly energy demand of between 2.5 to 3.2 TWh (SEAI, 2022).

8. Discussion

8.1. Other potential storage plays on the Irish Atlantic margin

There are several other storage plays that have been previously proposed as potential exploration targets during the search for hydrocarbon resources offshore Ireland. Both Amoco (1979) and the Petroleum Affairs Division (2005) noted the presence of high-quality reservoirs in the Scatálá and Siorc Sandstone Members at the base of the Lower Cretaceous Valhall Formation in the 12/13-1A well (Fig. 11), with log-derived porosities of 15-25% recorded (Amoco, 1979). The mudstones and marls of the surrounding Valhall Formation were inferred to seal these Cretaceous sandstone reservoirs. No indications of hydrocarbons were recorded in either sandstone member Amoco (1979). As this reservoir-seal pair has only been encountered in a single well in the study area, it is difficult to evaluate it further.

A second potential storage play in the study area is a fractured basement reservoir along the crest of the Erris Ridge (Fig. 16) similar to that proven on the Rona Ridge in the West of Shetland region (Holdsworth *et al.*, 2019). This would have consisted of a reservoir where porosity was provided primarily by fracture networks in the crystalline basement of the Erris Ridge, sealed by overlying Mesozoic mudstones. Howard *et al.* (2009) mentioned that an exploration well was planned to test this reservoir in 2010 but it was ultimately never drilled. At present too little data has been acquired to adequately assess either of these two storage plays and their potential utility as part of the storage portfolio for Ireland's energy future.

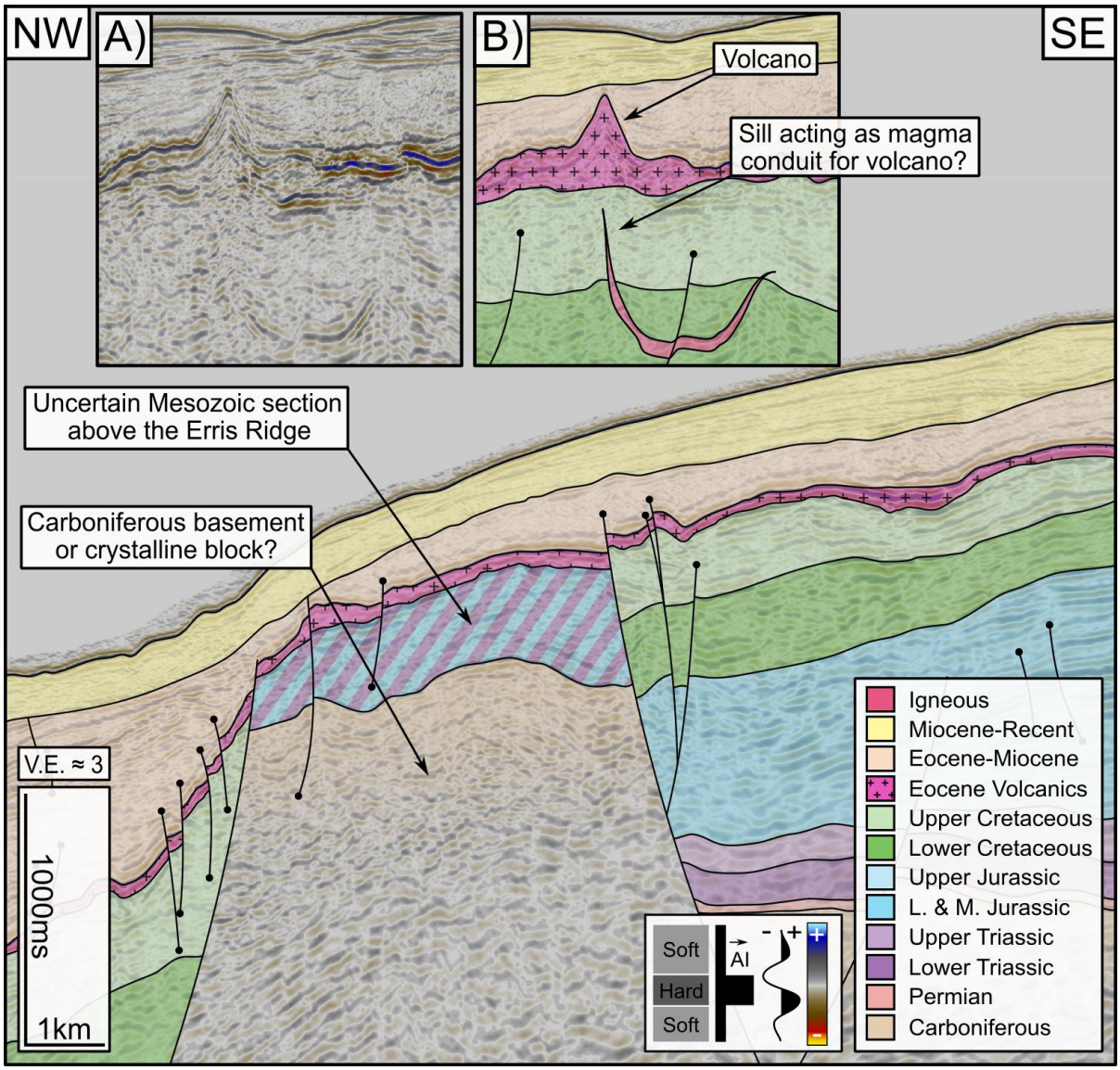

Figure 16: Geoseismic section through the Erris Ridge in the Northern Erris Sub-basin. A) Uninterpreted and B) Interpreted seismic section through a volcano, demonstrating the extrusion of the Eocene lavas and the possible link with underlying igneous intrusions. See Figure 2 for map location.

8.2. Salt cavern storage on the Irish Atlantic margin

There are two regionally extensive layers of salt present within the study area: the Permian Zechstein Group and the Upper Triassic Uilleann Halite Member (Merlin Energy Resources Consortium, 2020). The salt-prone Zechstein Group is present throughout the Slyne Basin and extends into the southern Erris Basin but becomes clastic- and carbonate-dominated in

the Northern Erris Sub-basin (Fig. 17). The Uilleann Halite Member is restricted to the Northern Slyne and Southern Erris sub-basins (Fig. 17; O'Sullivan *et al.*, 2021). While these layers of salt do not contain any natural reservoirs, man-made caverns can be created to produce gas storage sites and are commonly used across the world to store fluids in the subsurface (Casacão *et al.*, 2023; Ozarslan, 2012; Duffy *et al.*, 2022; Ramos *et al.*, 2022). The Zechstein Group consists of relatively clean halite and anhydrite with few interbedded insoluble sediments, with less than 2% and 6% insoluble material in the 27/5-1 and 18/25-2 wells respectively (Fig. 17). Conversely, the Uilleann Halite Member is interbedded with multiple layers of red mudstone with 12-13% insoluble material recorded in the 18/20-1 and 18/20-4 wells, although these are concentrated towards the top of the unit, with cleaner halite towards the base (Fig. 17). These impurities would result in a sump pile at the base of any cavern made in this salt layer, reducing the final volume. These interbedded layers of insoluble strata also represent zones of potential failure and leakage along the cavern walls (Bérest *et al.*, 2019; Duffy *et al.*, 2022).

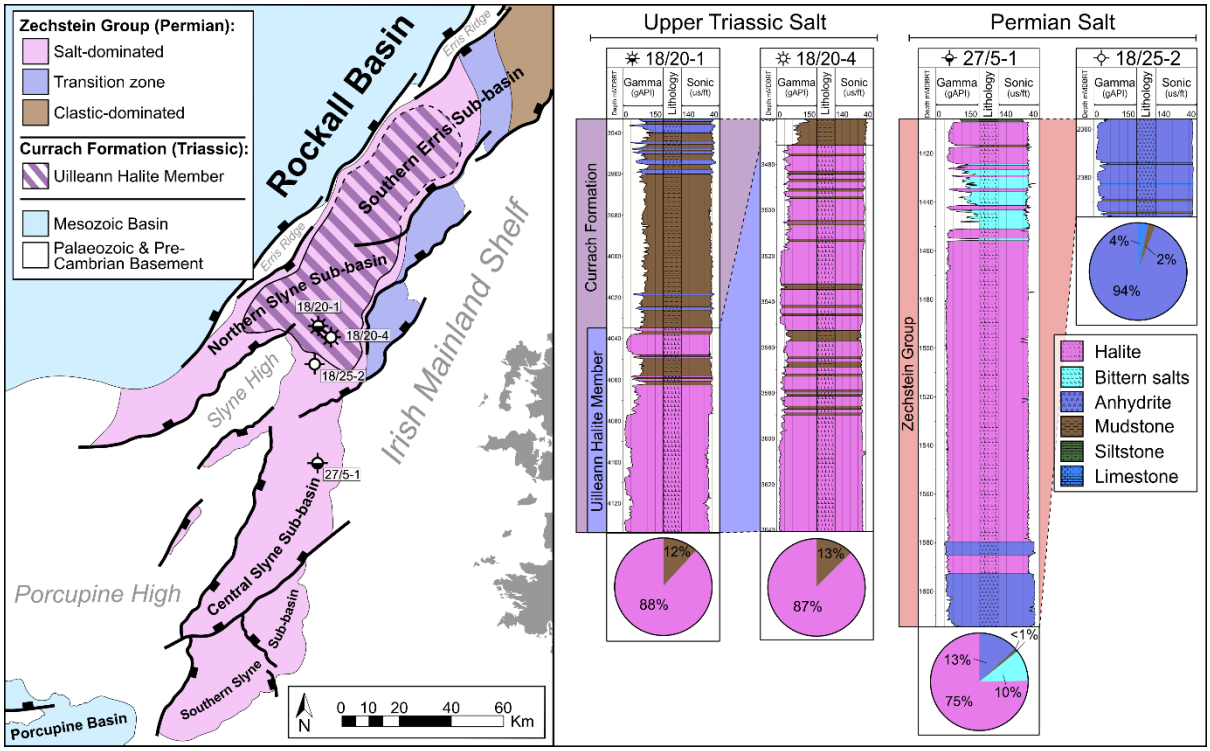

Figure 17: Map showing the distribution of Permian and Triassic salt within the Slyne and Erris basins alongside well sections comparing the composition of the Zechstein Group and the Uilleann Halite Member. Map adapted from O'Sullivan et al., 2021. Note on the wells displayed in the well correlation are shown on the map.

8.3. Comparison with basins offshore southern and eastern Ireland

As reference has been made to the basins offshore southern and eastern Ireland, for completeness, a brief comparison is made here with the Slyne, Erris and Donegal basins of the Irish Atlantic margin. These basins include the North and South Celtic Sea basins, the Central Irish Sea Basin and the Kish Bank Basin. These basins contain a sedimentary succession up to nine kilometres thick ranging from Permian to Cenozoic in age and which unconformably overlies a basement of Devonian to Carboniferous age (Rodriguez-Salgado *et al.*, 2020; Rowell, 1995; Shannon, 1991). The basins offshore southern and eastern Ireland evolved through multiple rift episodes during the Mesozoic and were later affected by basin

inversion and exhumation during the Cretaceous and Cenozoic, in a similar manner to those offshore northwest Ireland.

Several storage plays are present in the Celtic Sea basins. These include the Lower Triassic and Upper Jurassic storage plays discussed above which are common to both the Irish Atlantic margin and Celtic Sea basins. The limestones and sandstones of the Middle Jurassic Eagle Group and sandstones of the Lower Cretaceous Wealden and Selborne groups represent additional reservoirs, which are sealed by interbedded mudstones and the overlying Upper Cretaceous Chalk Group. These would form candidate Middle Jurassic and Lower Cretaceous storage plays respectively.

In both the Central Irish Sea and Kish Bank basins, multi-kilometre exhumation and erosion during the Cenozoic has removed any Cretaceous sediments, while only a thin veneer of Cenozoic sediments are present (Holford *et al.*, 2005, Murdoch *et al.*, 1995). Therefore, the Lower Cretaceous storage play of the Celtic Sea basins does not extend into the basins offshore eastern Ireland. Several other plays are present, including the Lower Triassic, Middle Jurassic and Upper Jurassic plays discussed previously. An additional storage play in the Central Irish Sea and Kish Bank basins include the Collyhurst Sandstone and Manchester Marl formations as a Lower and Upper Permian reservoir-seal pair respectively.

The multitude of storage plays present in the basins offshore southern and eastern Ireland are complemented by a variety of structural trap types including four-way dip closures, tilted fault blocks and salt-related folds (Fig. 18). Four-way dip closures are the most common structural trap type in the in Celtic Sea basins but are very uncommon in the Central Irish Sea and Kish Bank Basin. These structures formed in the hangingwalls of low-angle faults as a result of folding and reverse fault reactivation during the Middle Eocene (Rodriguez-Salgado *et al.*, 2020). These structures host three now-decommissioned gas fields (Kinsale, Ballycotton and Seven Heads, Fig. 18A) which had a total production of 53.8 Bcm, alongside several undeveloped gas accumulations (e.g. Galley Head, Schull, Carrigaline and Old Head). These hydrocarbon accumulations are primarily hosted in the Lower Cretaceous storage play. A recent study by Rodriguez-Salgado *et al.* (2022a) has estimated a capacity of 17611 Mt CO_2 in inversion structures in the Celtic Sea basins.

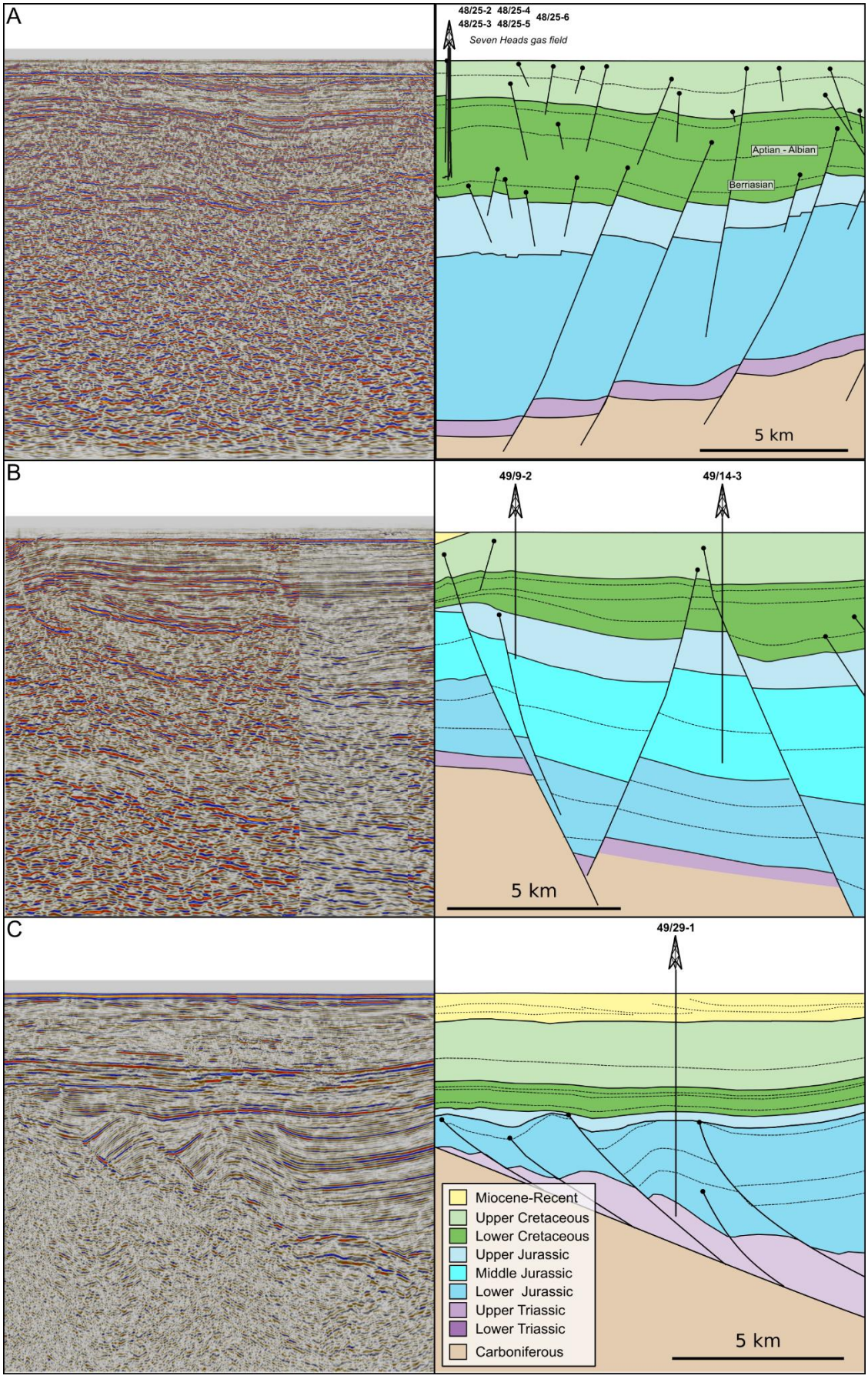
A
48/25-2 48/25-4
48/25-3 48/25-5 48/25-6
Seven Heads gas field
Aptian - Albian
Berriasian
5 km
B
49/9-2
49/14-3
5 km
C
49/29-1
Miocene-Recent
Upper Cretaceous
Lower Cretaceous
Upper Jurassic
Middle Jurassic
Lower Jurassic
Upper Triassic
Lower Triassic
Carboniferous
5 km

Figure 18: Examples of the main trap types observed in the basins offshore southern and eastern Ireland. A) Inversion structure (Seven Heads gas field), B) Tilted fault blocks (Helvick oil discovery) and C) Salt pillows.

Titled fault blocks are present throughout the basins offshore southern and eastern Ireland. In the North Celtic Sea Basin, the effectiveness of this trap type has been proven by the undeveloped Helvick oil discovery which consists of oil accumulations in four reservoir intervals in the Middle to Upper Jurassic (Fig. 18B; Caston, 1995). These tilted fault blocks formed during Triassic to Cretaceous rifting, while the normal faults bounding these structures were later reactivated with minor reverse motion (*i.e.* remaining net normal faults) during the Cenozoic (Rodríguez-Salgado *et al.*, 2022b).

Unlike the Slyne and Erris basins, only the Upper Triassic section contains salt in the basins offshore southern and eastern Ireland. These are the Feadóg Halite Member, restricted to the southern margin of the Celtic Sea basins, and the Warton Halite Formation in the Irish Sea respectively (Merlin Energy Resources Consortium, 2020). As in the Slyne and Erris basins, salt influences the evolution of structural traps due to its unique rheology. Where the salt is thickest it forms salt pillows and anticlines, folding the overlying layers to form salt-cored folds, during Triassic to Cretaceous rifting (Fig. 18C). Like the other structural traps discussed, these salt-related structures were later modified by reverse reactivation of the basin bounding faults during the Cenozoic. A faulted salt-cored structure on the Irish-UK maritime border hosts the undeveloped Dragon gas accumulation in Upper Jurassic sandstones and suggests these salt-cored structures could represent viable structural traps for subsurface gas storage.

The presence of proven seal and reservoir units, suitable trap structures proven to host hydrocarbon accumulations over geological timescales and their proximity to the Irish onshore, make the basins located in the Celtic and Irish Sea basins ideal locations for further investigation for gas storage alongside the basins of the Irish Atlantic margin.

8.4. Comparison with other methodologies applied to the Irish Atlantic margin

Two previous studies have assessed the potential of basins and structures on the Irish Atlantic margin for CO_2 storage: Lewis *et al.* (2009) and English and English (2022). Lewis *et al.* (2009) carried out an all-island assessment of the Upper Palaeozoic and Mesozoic basins located onshore and offshore Ireland. A large portion of the data available for this study was confidential at the time and so those authors classified the capacity for the Slyne and Erris basins as theoretical and did not provide a storage volume estimate (Lewis *et al.*, 2009). No reference was made to the Donegal Basin in that study. Lewis *et al.* (2009) used a modified GIP equation (*e.g.* Calhoun, 1976) for calculating saline aquifer capacity for other basins in the Irish and Celtic seas:

$$CO_2\ storage\ capacity = total\ pore\ volume\ \times density\ of\ CO_2\ \times 0.4$$

Total pore volume was calculated with an average porosity and net-to-gross values throughout the basin while using the whole area of the basin and an average reservoir thickness to calculate gross rock volume. The value of 0.4 accounts for the fluid dynamics of CO_2 resulting in relatively low gas saturation. While this method allows rapid estimation of the total potential capacity of a basin, it does not identify structural traps or account for lateral (*i.e.* net-to-gross) and vertical (*i.e.* porosity) changes in geology within the basin.

Both Lewis *et al.* (2009) and English and English (2022) applied the equation for depleted gas reservoirs presented by Bachu and Shaw (2003) for estimating CO_2 storage capacity in Ireland's gas fields:

$$CO_2\ storage\ capacity = \left({V_g(sc)}/{FVF}\right) \times density\ of\ CO_2$$

Where $V_g(sc)$ is the ultimate volume of recoverable gas at standard conditions and FVF is the gas formation volume factor, representing the ratio of volume at reservoir and standard conditions. Using this equation, English and English (2022) calculated a CO_2 capacity of 44 million tonnes for the Lower Triassic reservoir in the Corrib gas field, including a discount factor of 0.65 to account for water invasion during initial gas production. This is similar to the P50 value calculated in this study for the Corrib Triassic storage play using the initial gas-water contact as the closing contour (54 million tonnes, Table 2).

Recent publications have also investigated the potential of Ireland's sedimentary basins to host subsurface hydrogen storage sites (Dinh, *et al.*, 2021; Xiao *et al.*, 2022; English and English, 2023). These authors identified the geology of the basins offshore north-western Ireland as being suitable for further investigation. English and English (2023) also applied a modified version of Bachu and Shaw's (2003) equation for depleted gas fields to assess the volume of working gas capacity of the Corrib gas field. They calculated a similar value (37.7 TWh) to the P50 calculated for the Corrib Triassic storage play (Table 2) using the initial gas-water contact as the closing contour in this study (32 TWh).

The methods used in this study provide a greater degree of predictive power when it comes to estimating subsurface storage volumes in underexplored regions like the Irish Atlantic margin. The methods of Lewis *et al.* (2009) are most applicable in a basin-by-basin comparison for estimating basin-wide gas storage capacity but does not account for the lateral and vertical changes in intra-basinal geology and lacks the spill-point analysis component to identify structural closures within a particular basin. Bachu and Shaw's (2003) method for estimating volumes in depleted gas fields used by both Lewis *et al.* (2009) and English and English (2022) relies of existing developed gas accumulations, making it a very powerful tool in mature oil and gas provinces like the North Sea and East Irish Sea, but less so in underexplored areas like the sedimentary basins offshore Ireland.

8.5. Linking subsurface storage with other infrastructure on the Irish Atlantic margin

This study has primarily considered the geological factors influencing the suitability of different structures to act as subsurface storage sites. Alongside the geological characteristics discussed above, other considerations are important when considering the development of offshore storage facilities including the distance from potential offshore renewable energy generation sites, which may be producing excess energy to power a CAES system or generate hydrogen gas, or high CO_2 emitters. Two of Ireland's largest point-source CO_2 emitters (Moneypoint power station and Aughinish Alumina) are located on the western coast of the country (Table 5; Fig. 19; European Commission, 2022). Local storage plays in the Southern Slyne Sub-basin in particular (*e.g.* the Inishmore structure) may therefore make suitable storage locations for CO_2 generated from these large point-source emitters.

Table 5: 25 largest CO_2 emitters in Ireland in 2021 (European Commission, 2022). Note IDs 1, 18 and 19 are not point source emitters.

ID	Emitting entity	Type of activity	Verified emissions 2021 (tonnes of CO_2)
1	Ryanair DAC	Aircraft operator	4941568
2	ESB Moneypoint Generating Station	Coal-fired power station	3228756
3	Aughinish Alumina	Alumina refinery	1185891
4	Irish Cement Limited (Platin Works)	Cement manufacturer	1065759
5	Great Island Generating Station	CCGT power station	993092
6	Scotchtown Cement Works	Cement manufacturer	849233
7	Aghada CCGT	CCGT power station	807993
8	Huntstown Power Station	CCGT power station	775793
9	Tynagh 400MW CCPP	CCGT power station	773138
10	Irish Cement Limited (Limerick Works)	Cement manufacturer	766035
11	Dublin Bay Power Plant	CCGT power station	679932
12	ESB Poolbeg Generating Station (CCGT)	CCGT power station	659638
13	Tarbert Generating Station	Oil-fired power station	485972
14	Breedon Cement Ireland Limited	Cement manufacturer	453868
15	Edenderry Power Plant	Peat and biomass-fired power station	334945
16	Irving Oil Whitegate Refinery Limited	Oil refinery	294148
17	CCGT HPC2 (Huntstown Power Station Phase II)	CCGT power station	190841
18	Aer Lingus Limited AOHA	Aircraft operator	161319
19	ASL Airlines (Ireland) Limited	Aircraft operator	160526
20	Premier Periclase Limited	Magnesia-product manufacturer	104703
21	Glanbia Ireland DAC Ballyragget	Dairy products manufacturer	85471
22	Clogrennane Lime Limited (Toonagh Lime Works)	Lime manufacturer	82164
23	Bord na Mona Derrinlough Briquette Factory	Briquette manufacturer	75845
24	Bailieboro Foods Limited	Dairy products manufacturer	75139

25	Whitegate Power Station	CCGT power station	64239

The development of major offshore wind projects along Ireland's western and north-western coastlines (Fig. 19) may provide synergistic opportunities to explore the subsurface energy storage potential of the Slyne, Erris and Donegal basins. This could involve power-to-gas schemes, using excess electricity to generate either H_2 fuel or to inject compressed air into storage sites in these basins, providing deployable energy to meet national demand. These synergies have recently been explored in the North Sea and East Irish Sea basins in the UK and at the Kinsale Head gas field offshore southern Ireland (*e.g.* O'Kelly-Lynch *et al.*, 2020; Peecock *et al.*, 2023).

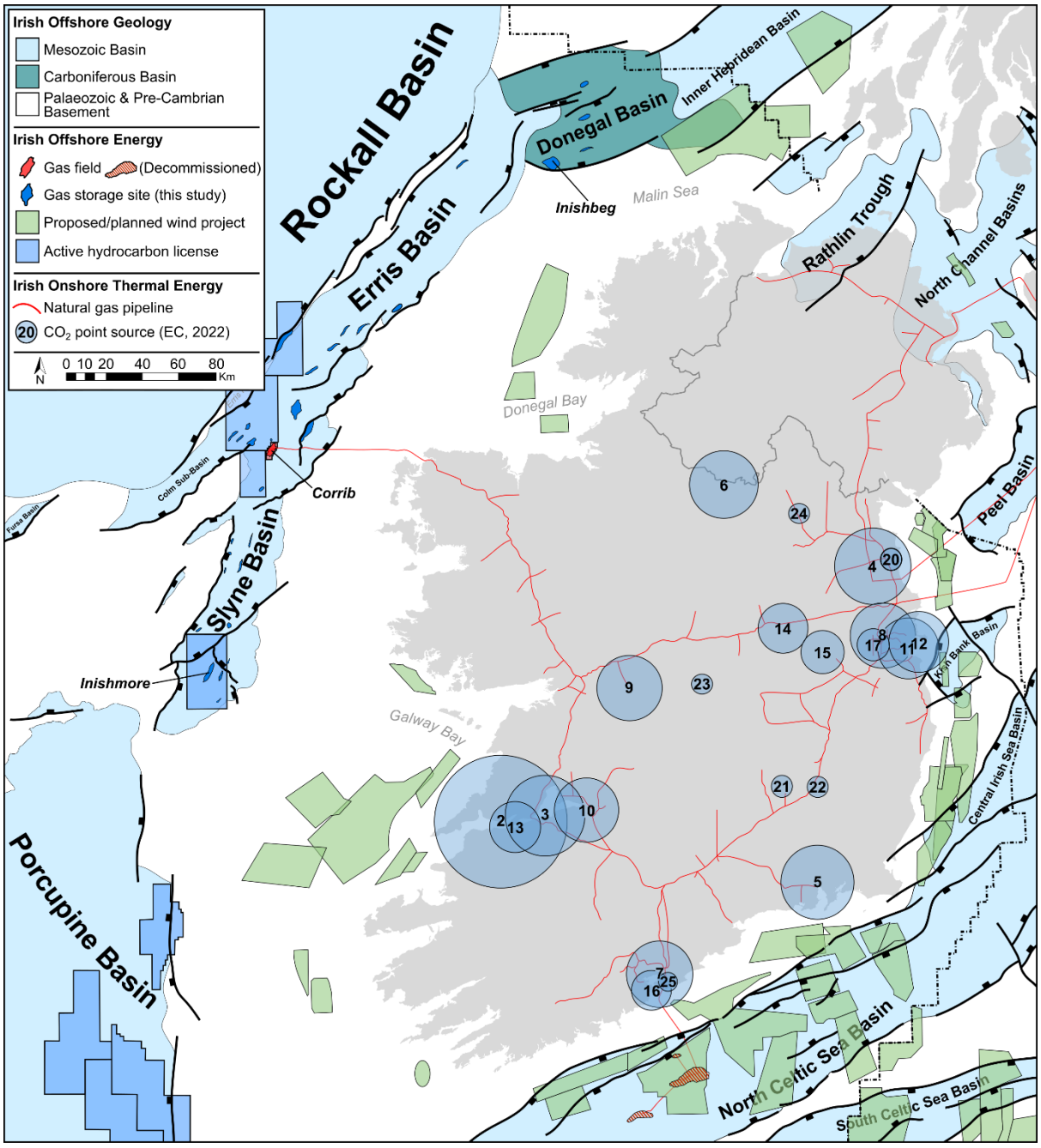

Figure 19: Overview map of energy infrastructure on- and offshore Ireland. Size of CO_2 point source emitters (note IDs 1, 18 and 19 are not point source emitters and are excluded here) proportional to scale

of emissions (see Table 5). CO_2 emission data and locations from European Commission, 2022. Proposed offshore wind development polygons are adapted from 4C Offshore, 2023. Celtic and Irish Sea basins adapted from Rodriguez-Salgado et al., 2022b. Porcupine Basin outline adapted from Saqab et al., 2020. Northern Irish and Scottish basins adapted from Fyfe et al., 2020.

These linked developments could include the proposed offshore wind developments to the west of the Shannon Estuary and Galway Bay and in Donegal Bay (Fig. 19; 4C Offshore, 2023). Offshore wind developments in Galway Bay could be connected to storage sites in the Southern and Central Slyne sub-basins, including the Inishmore structure analysed previously, while those in the Donegal Bay could be connected with storage sites in the Northern Slyne or Southern Erris sub-basins (Fig. 19). Offshore wind developments to the north of Ireland and the west of Scotland in the Malin Sea (Fig. 19; 4C Offshore, 2023) could be partnered with storage sites in the Donegal Basin including the Inishbeg storage site characterised in this study, through cross-border collaboration, or linked with structural closures identified in the Rathlin Trough and North Channel basins (*e.g.* Quinn *et al.*, 2010; Fyfe *et al.*, 2020).

The presence of existing subsea infrastructure will accelerate the development of offshore energy projects through reengineering and reuse. The decommissioned Kinsale Head gas field in the North Celtic Sea Basin (Fig. 19) is being actively investigated for its potential to store hydrogen gas with existing infrastructure (ESB, 2021). In the basins offshore north-western Ireland investigated in this study, the Corrib gas field represents one of the most attractive sites for further development as existing infrastructure can be repurposed for the storage and withdrawal of different gases when natural gas production finishes (*e.g.* DNV, 2021). This would significantly reduce capital expenditure when compared to a greenfield offshore storage site. Sites that are located near the Corrib gas field in the Northern Slyne Sub-basin and the Southern Erris Sub-basin could also benefit from their proximity of this existing infrastructure with development incentives similar to near-field exploration strategies employed in hydrocarbon exploration (*e.g.* Marchant *et al.*, 2001; Hulsey *et al.*, 2019). Therefore, it is likely that should gas storage sites be developed in the sedimentary basins offshore north-western Ireland, those near existing subsea infrastructure will be the first to be investigated.

9. Conclusions

A simplified workflow for estimating subsurface storage volumes has been developed that is scalable with different data densities. It can incorporate all available geological and engineering data to identify storage sites and estimate volumes. Estimates for storage volumes were calculated using a Gas In Place (GIP) equation for each gas type (CO_2 and H_2).

- Gross-rock-volume is calculated using top and base reservoir surfaces mapped on seismic reflection data and converted from the time to depth domain using time-depth relationship information from borehole checkshot surveys. Structural closures are then identified using a spill-point analysis technique.
- Net-to-gross is calculated using vshale curves, computed from gamma ray logs acquired in boreholes. This can be extrapolated regionally using a suitable geostatistical interpolation technique such as kriging to produce predictive regional net-to-gross maps.

- Porosity at depth is predicted using empirical compaction curves (*e.g.* Sclater & Christie, 1980) which best fit available porosity-depth information from cores, core plugs and cuttings. In the case study presented here from the Irish Atlantic margin, these curves were modified using local core and wireline data to account for regional erosion to avoid over estimation of porosity values.
- Theoretical gas saturations can be derived from laboratory studies of the relative permeabilities of the different gases relative to a saline formation water.
- The density of gases at reservoir conditions can be calculated using data derived from the pressure and temperature data extrapolated from wells in the study area. The density can be taken from an empirically derived database.

This is a suitable workflow to quickly identify a portfolio of prospective storage sites throughout a basin or group of basins that can scale from data-poor to data-dense areas. The identified storage sites can then be investigated with more detailed follow-up studies or additional data acquisition.

This workflow was then applied to the Slyne, Erris and Donegal basins offshore north-western Ireland, characterising three storage plays (an Upper Jurassic, Lower Triassic and Carboniferous play) and three candidate storage sites with varying levels of data coverage were investigated for their storage potential. These basins have geology that is favourable to their use in the storage of fluids. Each basin contains reservoir-seal pairs that have been locally proven in exploration wells alongside structural traps for gas storage. Amongst these basins, the Slyne Basin has the greatest density of subsurface data and is the most well-understood. The Currach and Corrib Sandstone formations make an ideal reservoir-seal pair, particularly where the Uilleann Halite Member is present towards the base of the Currach Formation.

As the development of the offshore wind resources on the west coast of Ireland proceeds, the case for further investigation and investment in these basins will strengthen. The Corrib gas field is an ideal candidate for further study on the feasibility of long-term storage of carbon dioxide in the Corrib Sandstone Formation, due to the wealth of subsurface data available and the presence of existing infrastructure.

Acknowledgements:

This research was funded in part by a research grant from Science Foundation Ireland (SFI) under Grant Number 13/RC/2092 and was co-funded under the European Regional Development Fund, and by the Petroleum Infrastructure Programme (PIP) and its member companies. Muhammad Mudasar Saqab and John Walsh are thanked for supervision during early stages of this project. The authors would like to thank the Petroleum Affairs Division (PAD) of the Department of Environment, Climate and Communications (DECC), Ireland, for providing access to seismic reflection and borehole datasets. Shell Exploration & Production Ireland Ltd. are thanked for providing access to reprocessed volumes of the 1997 Corrib 3D. The authors would also like to thank Schlumberger for providing academic licenses of Petrel to University College Dublin. SINTEF Digital is thanked for providing access to the open-source MRST-co2lab software. The colour maps used for surface elevation maps are developed by Fabio Crameri.

References:

4C Offshore. 2023. Global Offshore Renewable Database. Available at https://map.4coffshore.com/offshorewind/. Accessed 14/04/2023.

Agartan, E., Gaddipati, M., Yip, Y., Savage, B. and Ozgen, C. 2018. CO2 storage in depleted oil and gas fields in the Gulf of Mexico. International Journal of Greenhouse Gas Control, 72, 38–48, https://doi.org/10.1016/j.ijggc.2018.02.022.

Amoco 1978. Well 19/5-1 Geological Completion Report. Amoco Ireland Exploration Company, compiled by Odell, R.T. and Thomas, I.W.

Amoco 1979. Wells 12/13-1 and 12/13-1A Geological Completion Report. Amoco Ireland Exploration Company, compiled by Odell, R.T. and Walker, D.

Asquith, G., Krygowski, D., Henderson, S. and Hurley, N. 2004. Gamma Ray Log. In: Basic Well Log Analysis. 31–35., https://doi.org/10.1306/Mth16823C3.

Bachu, S. and Shaw, J. 2003. Evaluation of the CO2 Sequestration Capacity in Alberta's Oil and Gas Reservoirs at Depletion and the Effect of Underlying Aquifers. Journal of Canadian Petroleum Technology, 42, 51–61, https://doi.org/10.2118/03-09-02.

Bérest, P., Réveillère, A., Evans, D. and Stöwer, M. 2019. Review and analysis of historical leakages from storage salt caverns wells. *Oil & Gas Science and Technology – Revue d'IFP Energies Nouvelles*, **74**, 27, https://doi.org/10.2516/ogst/2018093.

Biancotto, F., Hardy, R.J.J., Jones, S.M., Brennan, D. and White, N.J. 2007. Estimating denudation from seismic velocities offshore NW Ireland. Society of Exploration Geophysicists – 77th SEG International Exposition and Annual Meeting, SEG 2007, 407–411.

Bickle, M.J. 2009. Geological carbon storage. Nature Geoscience, 2, 815–818, https://doi.org/10.1038/ngeo687.

Bui, M., Adjiman, C.S., Bardow, A., Anthony, E.J., Boston, A., Brown, S., Fennell, P.S, Fuss, S., Galindo, A., Hackett, L.A., Hallett, J.P., Herzog, H.J., Jackson, G., Kemper, J., Krevor, S., Maitland, G.C., Matuszewski, M., Metcalfe, I.S., Petit, C., Puxty, G., Reimer, J., Reiner, D.M., Rubin, E.S., Scott, S.A., Shah, N., Smit, B., Martin Trusler, J.P., Webley, P., Wilcox, J. and Mac Dowell, N. 2018. Carbon capture and storage (CCS): The way forward. Energy and Environmental Science, 11, 1062–1176, https://doi.org/10.1039/c7ee02342a.

Calhoun Jr, J.C. 1976. Fundamentals of reservoir engineering.

Casacão, J., Silva, F., Rocha, J., Almeida, J. and Santos, M. 2023. Aspects of salt diapirism and structural evolution of Mesozoic–Cenozoic basins at the West Iberian margin. AAPG Bulletin, 107, 49–85, https://doi.org/10.1306/08072221100.

Caston, V., 1995, The Helvick oil accumulation, Block 49/9, North Celtic Sea Basin: Geological Society, London, Special Publications, v. 93, no. 1, p. 209-225.

Chapman, T.J., Broks, T.M., Corcoran, D. V., Duncan, L.A. and Dancer, P.N. 1999. The structural evolution of the Erris Trough, offshore northwest Ireland, and

implications for hydrocarbon generation. Petroleum Geology of Northwest Europe: Proceedings of the 5th Conference, 455–469.

Corcoran, D.V. and Clayton, G. 2001. Interpretation of vitrinite reflectance profiles in sedimentary basins, onshore and offshore Ireland. Geological Society, London, Special Publications, 188, 61–90, https://doi.org/10.1144/GSL.SP.2001.188.01.04.

Corcoran, D.V. and Doré, A.G. 2002. Depressurization of hydrocarbon-bearing reservoirs in exhumed basin settings: evidence from Atlantic margin and borderland basins. Geological Society, London, Special Publications, 196, 457–483, https://doi.org/10.1144/GSL.SP.2002.196.01.25.

Corcoran, D.V. and Mecklenburgh, R. 2005. Exhumation of the Corrib Gas Field, Slyne Basin, offshore Ireland. Petroleum Geoscience, 11, 239–256, https://doi.org/10.1144/1354-079304-637.

Crotogino, F. 2022. Large-Scale Hydrogen Storage, https://doi.org/10.1016/B978-0-12-824510-1.00003-9.

Dancer, P.N., Algar, S.T. and Wilson, I.R. 1999. Structural evolution of the Slyne Trough. Petroleum Geology of Northwest Europe: Proceedings of the 5th Conference on the Petroleum Geology of Northwest Europe, 1, 445–454, https://doi.org/10.1144/0050729.

Dancer, P.N., Kenyon-Roberts, S.M., Downey, J.W., Baillie, J.M., Meadows, N.S. and Maguire, K. 2005. The Corrib gas field, offshore west of Ireland. Geological Society, London, Petroleum Geology Conference series, 6, 1035–1046, https://doi.org/10.1144/0061035.

Dawood, F., Anda, M. and Shafiullah, G.M. 2020. Hydrogen production for energy: An overview. International Journal of Hydrogen Energy, 45, 3847–3869, https://doi.org/10.1016/j.ijhydene.2019.12.059.

Dincer, I. 2012. Green methods for hydrogen production. International Journal of Hydrogen Energy, 37, 1954–1971, https://doi.org/10.1016/j.ijhydene.2011.03.173.

DNV. 2021. Re-Stream - Study on the Reuse of Oil and Gas Infrastructure for Hydrogen and CCS in Europe.

Dobson, M.R. and Whittington, R.J. 1992. Aspects of the geology of the Malin Sea area. *Geological Society, London, Special Publications*, **62**, 291–311, https://doi.org/10.1144/GSL.SP.1992.062.01.23.

Doré, A.G., Lundin, E.R., Jensen, L.N., Birkeland, O., Eliassen, P.E. and Fichler, C. 1999. Principal tectonic events in the evolution of the northwest European Atlantic margin. Petroleum Geology of Northwest Europe: Proceedings of the 5th Conference, 41–61.

Duffy, O.B., Hudec, M.R., Peel, F., Apps, G., Bump, A., Moscardelli, L., Dooley, T.P., Fernandez, N., Bhattacharya, S., Wisian, K. and Shuster, M.W. 2022. The Role of Salt Tectonics in the Energy Transition: An Overview and Future Challenges Running Title: Salt Tectonics and the Energy Transition. Tektonika, 1.

Dunford, G.M., Dancer, P.N. and Long, K.D. 2001. Hydrocarbon potential of the Kish Bank Basin: Integration within a regional model for the Greater Irish Sea Basin. Geological Society Special Publication, 188, 135–154, https://doi.org/10.1144/GSL.SP.2001.188.01.07.

Edwards BK. 2003. The economics of hydroelectric power.

Eiken, O., Ringrose, P., Hermanrud, C., Nazarian, B., Torp, T.A. and Høier, L. 2011. Lessons Learned from 14 years of CCS Operations: Sleipner, In Salah and Snøhvit. Energy Procedia, 4, 5541–5548, https://doi.org/10.1016/j.egypro.2011.02.541.

English, J. M., and English, K. L., 2022, Carbon Capture and Storage Potential in Ireland—Returning Carbon Whence It Came: First Break, v. 40, no. 5, p. 35-43.

Enterprise 1996a. Well IRE 27/5-1 Geological Completion Report. Enterprise Oil plc, compiled by Rawlinson, A., Verlander, J., Scotchman, I. and Henderson, G.

Enterprise 1996b. Well IRE 18/20-1 Geological Completion Report. Enterprise Oil plc, compiled by O'Neill, N., Scotchman, I. and Dancer, N.

Enterprise 2000. Well IRE 18/25-2 Geological Completion Report. Enterprise Oil plc, compiled by Pay, M. and Geerlings, P.

ESB. 2021. ESB and dCarbonX launch Kinsale Head Hydrogen Storage project. Available at: https://esb.ie/media-centre-news/press-releases/article/2021/08/12/esb-and-dcarbonx-launch-kinsale-head-hydrogen-storage-project/ . Accessed: 03/11/2022

European Commission. 2022. The EU emissions trading system (EU ETS). Directorate-General for Climate Action, Publications Office.

Fugro. 1994. Field Report Irish Frontier Shallow Coring Project Blocks 19/13 and 27/24 Irish Sector Atlantic Ocean (Volume II).

Fyfe, L.-J.C., Schofield, N., Holford, S.P., Heafford, A. and Raine, R. 2020. Geology and petroleum prospectivity of the Larne and Portpatrick basins, North Channel, offshore SW Scotland and Northern Ireland. Petroleum Geoscience, https://doi.org/10.1144/petgeo2019-134.

Garcia, X., Monteys, X., Evans, R.L. and Szpak, M. 2014. Constraints on a shallow offshore gas environment determined by a multidisciplinary geophysical approach: The Malin Sea, NW Ireland. Geochemistry, Geophysics, Geosystems, 15, 867–885, https://doi.org/10.1002/2013GC005108.

Godec, M., Kuuskraa, V., Van Leeuwen, T., Melzer, L.S. and Wildgust, N. 2011. CO2 storage in depleted oil fields: The worldwide potential for carbon dioxide enhanced oil recovery. Energy Procedia, 4, 2162–2169, https://doi.org/10.1016/j.egypro.2011.02.102.

Hashemi, L., Blunt, M. and Hajibeygi, H. 2021. Pore-scale modelling and sensitivity analyses of hydrogen-brine multiphase flow in geological porous media. Scientific Reports, 11, 1–13, https://doi.org/10.1038/s41598-021-87490-7.

Heinemann, N., Booth, M.G., Haszeldine, R.S., Wilkinson, M., Scafidi, J. and Edlmann, K. 2018. Hydrogen storage in porous geological formations – onshore play opportunities in the midland valley (Scotland, UK). International Journal of Hydrogen Energy, 43, 20861–20874, https://doi.org/10.1016/j.ijhydene.2018.09.149.

Holdsworth, R.E., McCaffrey, K.J.W., Dempsey, E., Roberts, N.M.W., Hardman, K., Morton, A., Feely, M., Hunt, J., Conway, A. and Robertson, A. 2019. Natural fracture propping and earthquake-induced oil migration in fractured basement reservoirs. Geology, 47, 700–704, https://doi.org/10.1130/g46280.1.

Holford, S. P., Turner, J. P., and Green, P. F. 2005. Reconstructing the Mesozoic–Cenozoic exhumation history of the Irish Sea basin system using apatite fission track analysis and vitrinite reflectance data. In Geological Society, London, Petroleum Geology Conference series (Vol. 6, No. 1, pp. 1095-1107). Geological Society of London.

Holloway, S., Vincent, C.J., Bentham, M.S. and Kirk, K.L. 2006. Top-down and bottom-up estimates of CO2 storage capacity in the United Kingdom sector of the southern North Sea basin. Environmental Geosciences, 13, 71–84, https://doi.org/10.1306/eg.11080505015.

Howard, A., Beswetherick, S. and Miglio, G. 2009. Prospectivity on the Erris Ridge (Licence 7/97)—High Risk/High Reward Frontier Exploration on the Irish Atlantic Margin. In: Offshore Europe, https://doi.org/10.2118/125073-MS.

Hudec, M.R. and Jackson, M.P.A. 2007. Terra infirma: Understanding salt tectonics. Earth-Science Reviews, 82, 1–28, https://doi.org/10.1016/j.earscirev.2007.01.001.

Hulsey, J., Bernaez, A., Strickland, B. and Cook, A. 2019. Workflows for near-field exploration. Interpretation, 7, T595–T606, https://doi.org/10.1190/INT-2018-0200.1.

Iglauer, S. 2022. Optimum geological storage depths for structural H2 geo-storage. Journal of Petroleum Science and Engineering, 212, 109498, https://doi.org/10.1016/j.petrol.2021.109498.

IPCC, 2022: Climate Change 2022: Mitigation of Climate Change. Contribution of Working Group III to the Sixth Assessment Report of the Intergovernmental Panel on Climate Change. P.R. Shukla, J. Skea, R. Slade, A. Al Khourdajie, R. van Diemen, D. McCollum, M. Pathak, S. Some, P. Vyas, R. Fradera, M. Belkacemi, A. Hasija, G. Lisboa, S. Luz, J. Malley, (eds.). Cambridge University Press, Cambridge, UK and New York, NY, USA. https://doi.org/10.1017/9781009157926

Jackson, M.P.A. and Hudec, M.R. 2017a. Salt Pillows and Salt Anticlines. *In*: *Salt Tectonics*. 62–75., https://doi.org/10.1017/9781139003988.007.

Jackson, M.P.A. and Hudec, M.R. 2017b. Salt Stocks and Salt Walls. *In*: *Salt Tectonics*. 76–118., https://doi.org/10.1017/9781139003988.008.

Klempa, M., Ryba, J. and Bujok, P. 2019. The storage capacity of underground gas storages in the Czech Republic. *GeoScience Engineering*, **65**, 18–25, https://doi.org/10.35180/gse-2019-0014.

Krevor, S.C.M., Pini, R., Zuo, L. and Benson, S.M. 2012. Relative permeability and trapping of CO2 and water in sandstone rocks at reservoir conditions. Water Resources Research, 48, 1–16, https://doi.org/10.1029/2011WR010859.

Lange, M., O'Hagan, A.M., Devoy, R.R.N., Le Tissier, M. and Cummins, V. 2018. Governance barriers to sustainable energy transitions – Assessing Ireland's capacity towards marine energy futures. Energy Policy, 113, 623–632, https://doi.org/10.1016/j.enpol.2017.11.020.

Lech, M.E., Jorgensen, D.C., Southby, C., Wang, L., Nguyen, V., Borissova, I. and Lescinsky, D. 2016. Palaeogeographic mapping to understand the hydrocarbon and CO2 storage potential of the post-rift Warnbro Group, offshore Vlaming Sub-basin, southern Perth Basin, Australia. Marine and Petroleum Geology, 77, 1206–1226, https://doi.org/10.1016/j.marpetgeo.2016.03.014.

Lewis, D., Bentham, M., Cleary, T., Vernon, R., O'Neill, N., Kirk, K., Chadwick, A., Hilditch, D., Michael, K., Allinson, G., Neal, P. and Ho, M. 2009. Assessment of the potential for geological storage of carbon dioxide in Ireland and Northern Ireland. Energy Procedia, 1, 2655–2662, https://doi.org/10.1016/j.egypro.2009.02.033.

Linstrom, P.J. and Mallard, W.G. 2022. NIST Chemistry WebBook, NIST Standard Reference Database Number 69, National Institute of Standards and Technology. https://doi.org/10.18434/T4D303

Lloyd, C., Huuse, M., Barrett, B.J. and Newton, A.M.W. 2021. Regional Exploration and Characterisation of CO2 Storage Prospects in the Utsira-Skade Aquifer, North Viking Graben, North Sea. Earth Science, Systems and Society, 1, 1–29, https://doi.org/10.3389/esss.2021.10041.

Lundin 2006. Well 13/12-1 Inishbeg Prospect End of Well Report. Lundin Britain Ltd., compiled by Craig, D. and Welding, P.

Maddox, S.J., Blow, R. and Hardman, M. 1995. Hydrocarbon prospectivity of the Central Irish Sea Basin with reference to Block 42/12, offshore Ireland. Geological Society Special Publication, 93, 59–77, https://doi.org/10.1144/GSL.SP.1995.093.01.08.

Marchant, T., Wilson, H. and Bamford, D. 2001. Near-Field Exploration: From Failure to Success. In: SPE Annual Technical Conference and Exhibition, https://doi.org/10.2118/71428-MS.

McVay, D.A. and Spivey, J.P. 2001. Optimizing Gas-Storage Reservoir Performance. *SPE Reservoir Evaluation & Engineering*, **4**, 173–178, https://doi.org/10.2118/71867-PA.

Merlin Energy Resources Consortium: The Standard Stratigraphic Nomenclature of Offshore Ireland: An Integrated Lithostratigraphic, Biostratigraphic and Sequence Stratigraphic Framework. Project Atlas. Petroleum Affairs Division, Department of the Environment, Climate and Communications, Special Publication 1/21. 2020.

Metz, B., Davidson, O., De Coninck, H.C., Loos, M. and Meyer, L. 2005. IPCC special report on carbon dioxide capture and storage. Cambridge: Cambridge University Press.

Miocic, J., Heinemann, N., Edlmann, K., Scafidi, J., Molaei, F. and Alcalde, J. 2023. Underground hydrogen storage: a review. Geological Society, London, Special Publications, 528, https://doi.org/10.1144/sp528-2022-88.

Møll Nilsen, H., Lie, K.-A., Møyner, O. and Andersen, O. 2015. Spill-point analysis and structural trapping capacity in saline aquifers using MRST-co2lab. Computers & Geosciences, 75, 33–43, https://doi.org/10.1016/j.cageo.2014.11.002.

Murdoch, L. M., Musgrove, F. W., and Perry, J. S. 1995. Tertiary uplift and inversion history in the North Celtic Sea Basin and its influence on source rock maturity. Geological Society, London, Special Publications, 93(1), 297-319.

Naylor, D. 1983. Petroleum exploration in the Republic of Ireland: A review. Energy exploration & exploitation, 3, 5–26.

Newborough, M. and Cooley, G. 2020. Developments in the global hydrogen market: The spectrum of hydrogen colours. Fuel Cells Bulletin, 2020, 16–22, https://doi.org/10.1016/S1464-2859(20)30546-0.

O'Kelly-Lynch, P., Gallagher, P., Borthwick, A., McKeogh, E. and Leahy, P. 2020. Offshore conversion of wind power to gaseous fuels: Feasibility study in a depleted gas field. Proceedings of the Institution of Mechanical Engineers, Part A: Journal of Power and Energy, 234, 226–236, https://doi.org/10.1177/0957650919851001.

Osmond, J.L., Mulrooney, M.J., Holden, N., Skurtveit, E., Faleide, J.I. and Braathen, A. 2022. Structural traps and seals for expanding CO2 storage in the northern Horda platform, North Sea. AAPG Bulletin, 106, 1711–1752, https://doi.org/10.1306/03222221110.

O'Sullivan, C. and Childs, C. 2021. Kinematic interaction between stratigraphically discrete salt layers; the structural evolution of the Corrib gas field, offshore NW Ireland. Marine and Petroleum Geology, 133, 105274, https://doi.org/10.1016/j.marpetgeo.2021.105274.

O'Sullivan, C.M., Childs, C.J., Saqab, M.M., Walsh, J.J. and Shannon, P.M. 2021. The influence of multiple salt layers on rift-basin development; The Slyne and Erris basins, offshore NW Ireland. Basin Research, 1–31, https://doi.org/10.1111/bre.12546.

O'Sullivan, C.M., Childs, C.J., Saqab, M.M., Walsh, J.J. and Shannon, P.M. 2022. Tectonostratigraphic evolution of the Slyne Basin. Solid Earth, 13, 1649–1671, https://doi.org/10.5194/se-13-1649-2022.

Ozarslan, A. 2012. Large-scale hydrogen energy storage in salt caverns. International Journal of Hydrogen Energy, 37, 14265–14277, https://doi.org/10.1016/j.ijhydene.2012.07.111.

Peecock, A., Edlmann, K., Mouli-Castillo, J., Martinez-Felipe, A. and McKenna, R. 2023. Mapping hydrogen storage capacities of UK offshore hydrocarbon fields and exploring potential synergies with offshore wind. Geological Society, London, Special Publications, 528, https://doi.org/10.1144/SP528-2022-40.

Petroleum Affairs Division. 2005. Petroleum Systems Analysis of the Slyne, Erris and Donegal Basins Offshore Ireland - Digital Atlas.

Philcox, M.E., Baily, H., Clayton, G. and Sevastopulo, G.D. 1992. Evolution of the Carboniferous Lough Allen Basin, Northwest Ireland. Geological Society Special Publication, 62, 203–215, https://doi.org/10.1144/GSL.SP.1992.062.01.18.

Pogge von Strandmann, P.A.E., Burton, K.W., Snæbjörnsdóttir, S.O., Sigfússon, B., Aradóttir, E.S., Gunnarsson, I., Alfredsson, H.A., Mesfin, K.G., Oelkers, E.H. and Gislason, S.R. 2019. Rapid CO2 mineralisation into calcite at the CarbFix storage

site quantified using calcium isotopes. Nature Communications, 10, 1983, https://doi.org/10.1038/s41467-019-10003-8.

PSE Kinsale Energy. 2020. Gas Storage. PSE Kinsale Energy, 22 August 2022. https://www.kinsale-energy.ie/gas-storage. Accessed 19 September 2022.

Quinn, M.F., Smith, K. and Bulat, J. 2010. A geological interpretation of the nearshore area between Belfast Lough and Cushendun, Northern Ireland, utilising a newly acquired 2D seismic dataset to explore for salt layers for possible gas storage within man-made caverns. British Geological Survey Commissioned Report, CR/10/069.

Ramos, A., García-Senz, J., Pedrera, A., Ayala, C., Rubio, F., Peropadre, C. and Mediato, J.F. 2022. Salt control on the kinematic evolution of the Southern Basque-Cantabrian Basin and its underground storage systems (Northern Spain). Tectonophysics, https://doi.org/10.1016/j.tecto.2021.229178.

Rezaei, A., Hassanpouryouzband, A., Molnar, I., Derikvand, Z., Haszeldine, R.S. and Edlmann, K. 2022. Relative Permeability of Hydrogen and Aqueous Brines in Sandstones and Carbonates at Reservoir Conditions. Geophysical Research Letters, 49, https://doi.org/10.1029/2022gl099433.

Ringrose, P. 2020. How to store CO2 underground: Insights from early-mover CCS projects. Springer Briefs in Earth Science **129**. Springer Cham. https://doi.org/10.1007/978-3-030-33113-9

Rodríguez-Salgado, P., Childs, C., Shannon, P.M. and Walsh, J.J. 2020. Structural evolution and the partitioning of deformation during basin growth and inversion: A case study from the Mizen Basin Celtic Sea, offshore Ireland. Basin Research, 1–24, https://doi.org/10.1111/bre.12402.

Rodriguez-Salgado, P., Walsh, J. J., Childs, C., and Manzocchi, T. 2022a. Unlocking the CO2 storage potential of the Celtic Sea Basins from hydrocarbon exploration legacy data, in Proceedings 83rd EAGE Conference & Exhibition 2022, Madrid, Spain.

Rodríguez-Salgado, P., Childs, C., Shannon, P.M. and Walsh, J.J. 2022b. Influence of basement fabrics on fault reactivation during rifting and inversion: a case study from the Celtic Sea basins, offshore Ireland. Journal of the Geological Society, 180, 315–338, https://doi.org/10.1144/jgs2022-024.

Roux, J.P., Fitch-Roy, O., Devine-Wright, P. and Ellis, G. 2022. “We could have been leaders”: The rise and fall of offshore wind energy on the political agenda in Ireland. Energy Research and Social Science, 92, 102762, https://doi.org/10.1016/j.erss.2022.102762.

Rowell, P., 1995, Tectono-stratigraphy of the North Celtic Sea Basin: Geological Society, London, Special Publications, v. 93, no. 1, p. 101-137.

Saqab, M.M., Childs, C., Walsh, J. and Delogkos, E. 2020. Multiphase deformation history of the Porcupine Basin, offshore west Ireland. Basin Research, 1–22, https://doi.org/10.1111/bre.12535.

Sclater, J.G. and Christie, P.A.F. 1980. Continental stretching: An explanation of the Post-Mid-Cretaceous subsidence of the central North Sea Basin. Journal of

Geophysical Research: Solid Earth, 85, 3711–3739, https://doi.org/10.1029/JB085iB07p03711.

Scotchman, I.C. and Thomas, J.R.W. 1995. Maturity and hydrocarbon generation in the Slyne Trough, northwest Ireland. The Petroleum Geology of Ireland's Offshore Basins, 93, 385–412, https://doi.org/10.1144/GSL.SP.1995.093.01.30.

Scotchman, I.C., Doré, A.G. and Spencer, A.M. 2018. Petroleum systems and results of exploration on the Atlantic margins of the UK, Faroes & Ireland: what have we learnt? Geological Society, London, Petroleum Geology Conference series, 8, 187–197, https://doi.org/10.1144/PGC8.14.

SEAI, 2022. Energy in Ireland 2022 Report. Sustainable Energy Authority of Ireland.

Serica Energy, 2009. Well 27/4-1, 1z Bandon exploration well and sidetrack geological end of well report. Serica Energy plc.

Shannon, P. 1991. The development of Irish offshore sedimentary basins: Journal of the Geological Society, v. 148, no. 1, p. 181-189.

Shannon, P.M. and Naylor, D. 1998. An assessment of Irish offshore basins and petroleum plays. Journal of Petroleum Geology, 21, 125–152, https://doi.org/10.1306/BF9AB7A1-0EB6-11D7-8643000102C1865D.

Shannon, P.M. 2018. Old challenges, new developments and new plays in Irish offshore exploration. Geological Society, London, Petroleum Geology Conference series, 8, 171–185, https://doi.org/10.1144/PGC8.12.

Span, R. and Wagner, W. 1996. A new equation of state for carbon dioxide covering the fluid region from the triple-point temperature to 1100 K at pressures up to 800 MPa. Journal of Physical and Chemical Reference Data, 25, 1509–1596, https://doi.org/10.1063/1.555991.

Spencer, A.M. and MacTiernan, B. 2001. Petroleum systems offshore western Ireland in an Atlantic margin context. Geological Society, London, Special Publications, 188, 9–29, https://doi.org/10.1144/GSL.SP.2001.188.01.02.

Statoil 2004. Well 19/11-1 & 1A Final Well Report. Statoil Exploration (Ireland) Ltd., compiled by Hofsøy, R., Skagen, J., Mortensen, H. and Conroy, J.

StatoilHydro 2009. Well 19/8-1 Cashel Prospect End of Well Report. Statoil Exploration (Ireland) Ltd., compiled by MacTiernan, B., Kleppa, S., Hunnes, O., Sigve-Selnes, K. and Igbineweka, O.J.

Takahashi, T., Ohsumi, T., Nakayama, K., Koide, K. and Miida, H. 2009. Estimation of CO2 Aquifer Storage Potential in Japan. Energy Procedia, 1, 2631–2638, https://doi.org/10.1016/j.egypro.2009.02.030.

Tate, M.P. and Dobson, M.R. 1989. Pre-Mesozoic geology of the western and north-western Irish continental shelf. *Journal of the Geological Society*, **146**, 229–240, https://doi.org/10.1144/gsjgs.146.2.0229.

Texaco 1978. Well 13/3-1 Final Geological Report. Texaco Ireland Ltd., compiled by Stuart, I.A.

Thiyagarajan, S.R., Emadi, H., Hussain, A., Patange, P. and Watson, M. 2022. A comprehensive review of the mechanisms and efficiency of underground hydrogen

storage. Journal of Energy Storage, 51, 104490, https://doi.org/10.1016/j.est.2022.104490.

Trueblood, S. 1992. Petroleum geology of the Slyne Trough and adjacent basins. Geological Society Special Publication, 315–326, https://doi.org/10.1144/GSL.SP.1992.062.01.24.

Tyrrell, S., Haughton, P.D.W. and Daly, J.S. 2007. Drainage reorganization during breakup of Pangea revealed by in-situ Pb isotopic analysis of detrital K-feldspar. Geology, 35, 971–974, https://doi.org/10.1130/G4123A.1.

Dinh, V.N., Leahy, P., McKeogh, E., Murphy, J. and Cummins, V. 2021. Development of a viability assessment model for hydrogen production from dedicated offshore wind farms. International Journal of Hydrogen Energy, 46, 24620–24631, https://doi.org/10.1016/j.ijhydene.2020.04.232.

Wall, F., Rollat, A. and Pell, R.S. 2017. Responsible sourcing of critical metals. Elements, 13, 313–318, https://doi.org/10.2138/gselements.13.5.313.

Woodcock, N. and Strachan, R. (eds). 2012. *Geological History of Britain and Ireland*, 2nd ed., https://doi.org/10.1002/9781118274064.

Worthington, R.P. and Walsh, J.J. 2011. Structure of Lower Carboniferous basins of NW Ireland, and its implications for structural inheritance and Cenozoic faulting. Journal of Structural Geology, 33, 1285–1299, https://doi.org/10.1016/j.jsg.2011.05.001.

Xiao, Z., Desmond, C., Stafford, P., and Li, Z. 2022. Geological perspectives of offshore underground hydrogen storage in Ireland, EGU General Assembly 2022, Vienna, Austria, 23–27 May 2022, EGU22-1645, https://doi.org/10.5194/egusphere-egu22-1645.

Yekta, A.E., Manceau, J.C., Gaboreau, S., Pichavant, M. and Audigane, P. 2018. Determination of Hydrogen–Water Relative Permeability and Capillary Pressure in Sandstone: Application to Underground Hydrogen Injection in Sedimentary Formations. Transport in Porous Media, 122, 333–356, https://doi.org/10.1007/s11242-018-1004-7.

Ziegler, P.A. 1992. North Sea rift system. *Geodynamics of Rifting*, **208**, 55–75, https://doi.org/10.1016/b978-0-444-89912-5.50007-7.